Friction in a solid lubricant film

O. M. Braun[1,*] and M. Peyrard[2]
[1]*Institute of Physics, National Ukrainian Academy of Sciences, 03650 Kiev, Ukraine*
[2]*Laboratoire de Physique de l'Ecole Normale Supérieure de Lyon, 46 Allée d'Italie, 69364 Lyon Cédex 07, France*
(Received 26 April 2000; published 28 March 2001)

Molecular-dynamics study of a thin (one to five layers) lubricant film between two substrates in moving contact are performed using Langevin equations with an external damping coefficient depending on distance and velocity of atoms relative the substrates, motivated by microscopic configurations. They show that the minimal friction coefficient is obtained for the solid-sliding regime. A detailed analysis of the results, the comparison with other microscopic modeling approaches of friction, and the evaluation of quantities that can be compared to experiments, such as the velocity of the transition from stick slip to smooth sliding, are used to discuss the relevance of the microscopic simulations of friction.

DOI: 10.1103/PhysRevE.63.046110 PACS number(s): 81.40.Pq, 46.55.+d, 61.72.Hh

I. INTRODUCTION

The problem of friction between two substrates which are in moving contact is very important technologically as well as very rich physically [1–7]. Following the development of atomic force microscopy, tribology has approached the microscopic level and these studies are expanding because nanotechnology is now building devices that are so miniaturized that they begin to probe the microscopic properties of the materials. But the atomic friction microscope has its own difficulties, in particular for ''high-speed friction,'' because it does not operate at high velocities. This explains the interest of numerical simulations of friction [8] (see also the review paper [7] and references therein). Moreover molecular dynamics can provide detailed information on the motion of individual atoms that help in the understanding of the basic mechanisms of friction, a problem which is still open in spite of the efforts devoted to it in the last few years. Unfortunately, large-scale simulation of dynamical processes with three-dimensional models and realistic interatomic potentials are still too time consuming for large systems, mainly due to slow relaxation processes in such systems. Moreover, the standard molecular-dynamics methods consider the atomic degrees of freedom only and ignore the electronic ones, that may be a too crude approximation in modeling metal substrates. Therefore, one has to use simplified models such as two-dimensional [9–11] or even one-dimensional [12,13] ones.

An intermediate complexity model, where a few atomic-layer film are placed between two rigid substrates so that the top and bottom lubricant layers may stick to the substrates while leaving mobile atoms in between, was analyzed in a series of papers [14,16–20] and also in our previous publications for commensurate [21] and incommensurate [22] lubricant films. Thermal equilibrium was achieved with the help of Langevin equations with a random Gaussian force and a viscous damping with a constant coefficient η. The Langevin thermostat was applied either to all degrees of freedom of the system [21,22], or only to the ones perpendicular to the sliding direction [14,16–20]. Owing to the relative simplicity of such models they allow the simulation of friction for a broad range of parameters and the study of general trends and laws of the phenomena. The main results obtained in these studies are the following. First, it was shown that the static frictional force f_s for the contact of bare substrates is very small in most cases, except in the rare situation in which the two surfaces are commensurate and perfectly aligned [7,23,24]. However, even a submonolayer of mobile atoms between the surfaces leads to a finite f_s that is proportional to the applied load and is almost independent of the system parameters [14]. Second, a thin lubricant film (with a thickness smaller than ~ 10 molecular diameters) confined between two solids is always layered and often solidified because the confinement decreases the entropy of the film and shifts the bulk melting transition to higher temperatures and lower pressures (see, e.g., Ref. [7] and references therein). This effect is even observed in equilibrium situations for highly confined films [15]. Third, when an external force f drives one of the substrates and it starts to move, the lubricant film melts and its width increases by $\sim 10\%$ [16,17]. After the shear-induced first-order melting transition, the lubricant exhibits a layer-over-layer sliding with strong two-dimensional order within shearing planes of atoms, where each layer moves coherently as a whole [17,22]. If then the driving force or velocity decreases back to a smaller value, the film solidifies again either in the solid state in the case of spherical molecules, or in an amorphous (glassy) phase for the case of lubricant consisting of long-chain (organic) molecules [18]. Thus, if the top substrate is coupled through a spring to a stage moving with a constant velocity, then at the beginning, the spring stretches and the force increases. Eventually f exceeds f_s, the top substrate begins to slide, and the lubricant melts. Then the top substrate accelerates to catch up with the stage and f decreases, so the substrates stick again. This periodic melting-freezing process was used by Thompson and Robbins [16] for explanation of the stick-slip motion observed experimentally. Fourth, when the film consists of flexible chain molecules, it may be trapped in a glassy state, and the sliding occurs only at the lubricant substrate interfaces (the pluglike flow) [18]. This explains why the effective viscosities of thin films may

*Electronic address: obraun@iop.kiev.ua

rise more than five orders of magnitude above bulk values (experimentally, the relaxation times are fractions of a second for thin confined films and nanoseconds for a bulk). Finally, the regime of smooth sliding with atomic-scale velocities was studied in Refs. [19,21,22]. It was shown that the kinetic frictional force can be described by the introduction of a phenomenological parameter that describes an ''intrinsic'' damping within the lubricant due to anharmonic coupling between its different modes. Also, in a recent paper [20] He and Robbins studied the friction at low velocities. Their simulations lead to a frictional force which is proportional to the load in accordance with the Amontons law, and rises logarithmically with velocity, again in agreement with experiments. The simulation results were explained as thermally activated motion of the lubricant over the periodic substrate potential.

However, all these studies raised the question of the validity of results obtained with simple models, in particular which results are of general validity and which ones are model dependent, and to what extend the results obtained on microscopic samples can be used to analyze actual experiments performed on a macroscopic scale. We think that these questions are important for the future of molecular-dynamics simulations of friction, and we want to address some aspects of them in the present paper.

A critical question is the energy flow out of the friction zone and the way it is described in the models because it governs the value of the friction coefficient. Thermal equilibrium is rather easy to simulate correctly because it does not depend on the value of the external damping η in Langevin equations or on the method used to introduce the damping (although the rate of approach to equilibrium depends on η). It is clear, however, that the nonequilibrium state of a system driven by an external dc force must depend on the method used to take into account the energy exchange with the outside, for instance on the type of external damping which is assumed. One may predict that the dependence is not crucial if the rate of energy exchange between different modes of the system, which emerges due to nonlinearity of the equations of motion, is (much) larger than energy transfered outside of the system, described by the external damping η. This case corresponds, for example, to a lubricant close to the melting temperature studied in Refs. [14,16–20], especially for lubricants with complex (long-chain) molecules. But for a monatomic lubricant or a lubricant with simple molecules at low temperatures and low driving velocities, when the lubricant film is in the solid state, the simulation results may strongly depend on the external damping. In the present paper we investigate this question by using a realistic energy-loss mechanism. Comparing with models previously used in friction simulation (as discussed above, see also Ref. [7] and references therein), the main new feature of the present paper is that we use Langevin equations with an external damping coefficient $\eta(z,v)$ which depends on the distance z of a lubricant atom from the substrate and on its velocity v with respect the substrate. Some significant differences with simpler modeling of the energy losses are exhibited.

With this model, we pay particular attention to the motion at small velocity v_{top} of the top substrate, looking for the smallest possible value of the velocity for which the motion stays smooth. We show that the microscopic transition from smooth sliding to stick-slip motion takes place at a velocity that is *many orders of magnitude higher than that observed in macroscopic experiments.* This is an important point in the connection between simulations and experiments, which suggests that the macroscopic mechanism of the transition from stick-slip motion to smooth sliding is completely different from the microscopic one.

We also used our extended model to examine various aspects of friction, which will be presented in the result and discussion sections. The paper is organized as follows. First, in Sec. II we describe the model and the algorithm used in the simulations, and we introduce an external damping coefficient for Langevin equations, based on microscopic considerations, which attempts to describe the energy exchange between the lubricant atoms and the substrates in a realistic way. Then in Sec. III we present the simulation results and analyze them considering the excitation of vibrations in the system. Finally, Sec. IV discusses the applicability of microscopic simulation to macroscopic experiments.

II. MODEL

We are interested in the regime of boundary lubrication, when two sliding surfaces come in solid contact, and in the contact region, the surfaces are separated by at most a *few* layers of lubrication molecules. We consider a model with a thin (one to five layers) *solid* lubricant film between two solids. There are two reasons for this choice. *First*, there is always some lubricant (called ''third bodies'' by tribologists) between the surfaces. It may correspond either to a specially chosen lubricant, or to water or other material adsorbed from air, a dust, grease, wear debris produced by sliding, etc. In general the lubricant is not commensurate with the substrates, and, even if they are commensurate, the lubricant and substrates are seldom perfectly aligned. The external load squeezes the lubricant out from the contact area, so a very thin lubricant film is often formed. The last layer is however very difficult to remove [3,25] so that there is at least one lubricant layer between the substrates. Due to the load, the lubricant is always strongly compressed and thus has to form a closely packed structure. As a result, the confined thin film solidifies [7,18] as was mentioned above. *Second*, we are interested in low friction situations, and it is in the case of a solid thin lubricant film that we may expect to obtain the minimal friction. When the lubricant is liquid or amorphous, the kinetic friction is usually much larger [4–6,19,26].

Moreover, contrary to our previous studies [21,22], now the surface layers of the substrates are simulated directly. The substrates consists of two parts. A rigid part forms the boundaries of the model system, and a deformable substrate layer is in contact with the lubricant, providing a much more realistic description of the substrate than previously.

Our three-dimensional system comprises a few atomic-layer film between two parallel rigid top and bottom substrate parts as shown in Fig. 1. Each rigid substrate part has $N_S=132$ atoms henceforth called s atoms organized into a 12×11 lattice of square symmetry with the lattice constant

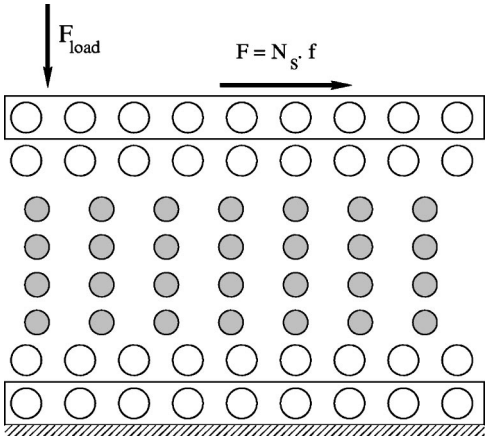

FIG. 1. Schematic picture of the model. The gray circles show the lubricant atoms, while open circles show the substrate atoms. The enclosed atoms in the two substrates correspond to the rigid parts of the substrate while the dynamics of the other substrate atoms is fully simulated. The load and shear forces are applied to the rigid part of the top substrate as shown by the arrows. The rigid part of the bottom substrate is fixed.

$a_s=3$. The atoms of the bottom rigid substrate part are fixed while the top substrate part moves rigidly. Between the rigid substrate parts we insert atoms of two different kinds: $2N_S$ *s* atoms model the surfaces of the substrate, which are therefore modeled more accurately than with rigid body, and $N_{al}N_l$ *l* atoms (''lubricant'' atoms) form the lubricant film. In the *x* and *y* directions we use periodic boundary conditions. The top substrate part and all the atoms may move in all three dimensions. To shorten the expressions we henceforth call top and bottom ''substrates'' the rigid parts of the substrates. It should be kept in mind that these ''substrates'' are in fact only a part of the top and bottom solids that slide on each other. All atoms interact via a 6-12 Lennard-Jones pairwise potential

$$V(r)=V_{\alpha\alpha'}\left[\left(\frac{r_{\alpha\alpha'}}{r}\right)^{12}-2\left(\frac{r_{\alpha\alpha'}}{r}\right)^{6}\right], \tag{1}$$

but the parameters of the potential (1) are different for different kinds of atoms. For the *s*-*s* interaction we took $V_{ss}=3$ and $r_{ss}=3$, for the *l*-*l* interaction, $V_{ll}=1$ and $r_{ll}=4.14$ (''incommensurate'' case), and for the *s*-*l* interaction, $V_{ls}=1/3$ (corresponding to a weak interaction between the substrate and the lubricant) and $r_{ls}=\frac{1}{2}(r_{ss}+r_{ll})=3.57$, respectively. The cutting radius for the interaction was chosen as $r^*=1.49\,r_{ll}=6.17$. With these energy parameters, the *S* atoms stick to the top and bottom substrates, covering them with monolayers, while the *l* atoms fill the space between the substrates. This simulates a lubricant between two solids, and the surface (utmost) layer of each substrate is treated explicitly. The equilibrium configuration of the lubricant corresponds to N_l layers, each having $N_{al}=80$ atoms, organized into a close-packed triangular lattice slightly distorted by the substrate potentials.

For the masses we took $m_l=m_s=m_S=1$, which gives a typical frequency for the system of $\omega_s=[V''_{ss}(r_{ss})/m_s]^{1/2}=4.9$, and the corresponding characteristic period is $\tau_s=2\pi/\omega_s=1.28$. A typical frequency of vibrations within the lubricant is $\omega_l=6(2V_{ll}/m_l r_{ll}^2)^{1/2}=2.05$. To each atom of the top rigid substrate we apply a dc force consisting of a driving force *f* along the *x* axis and a loading force $f_{\rm load}=-0.1$ along the *z* direction. These parameters have been used in most of the simulations, except when otherwise specified.

Units. Although we work with dimensionless quantities, the numerical values of the model parameters have been chosen such that, if energy were measured in electron volts and distances in Angströms, we would have realistic values for a typical solid. However, for a discussion of the applicability of simulations to real physical systems, it is useful to couple the ''natural units'' (nu) used in the simulation with, e.g., the Systeme International (International System of units). The basic parameters that were unchanged in all simulations, are the amplitude of interaction within the substrates ($V_{ss}=3$), which sets the energy parameter, the substrate lattice constant ($a_s=3$) that sets the length scale, and the mass of lubricant atoms ($m_l=1$) as the mass parameter. A real system can be characterized by the amplitude of interaction in the substrates $\tilde{V}_{ss}$ measured in eV, by the substrate lattice constant $\tilde{a}_s$ measured in Å , and by the mass of lubricant atoms $\tilde{m}_l$ measured in proton masses m_p. If we introduce the following coefficients, $\nu_e=\tilde{V}_{ss}/V_{ss}=\tilde{V}_{ss}/3$, $\nu_r=\tilde{a}_s/a_s=\tilde{a}_s/3$, and $\nu_m=\tilde{m}_l/(100\,m_l)=\tilde{m}_l/100$, then for a typical system we have $\nu_e\sim\nu_r\sim\nu_m\sim 1$, and it is easy to find these coefficients for a real physical system.

Now we can couple our natural units with the SI system of units. Namely, we have for the unit of length 1 *m* $=10^{10}\,\nu_r^{-1}$ nu, for the unit of mass 1 kg$=6\times10^{24}\,\nu_m^{-1}$ nu, for the unit of energy 1 *J*$=6.25\times10^{18}\,\nu_e^{-1}$ nu, for the unit of force 1 N$=6.25\times10^{8}\,(\nu_r/\nu_e)$ nu, for the unit of pressure 1 N/m$^2=6.25\times10^{-12}\,(\nu_r^3/\nu_e)$ nu, for the unit of time 1 *s* $=0.98\times10^{13}(\nu_e/\nu_m\nu_r^2)^{1/2}$ nu, and for the unit of velocity 1 m/s$=1.02\times10^{-3}(\nu_m/\nu_e)^{1/2}$ nu. In particular, the load force $f_{\rm load}=-0.1$ nu. used in the simulations, corresponds to the pressure $P=-f_{\rm load}/a_s^2=1.11\times10^{-2}$ nu$=1.78\times10^{9}$ N/m^2. To compare with experimentally used values, note that a realistic pressure is $P\sim10^7$ N/m^2, and the maximum pressure above which the plastic deformation begins, is $P\approx2\times10^8$ N/m^2 for gold (a minimal value for metals), $P\approx10^9$ N/m^2 for steel, and $P\approx10^{11}$ N/m^2 for diamond (the largest possible value). As for velocities, a typical value when the transition from a stick-slip motion to smooth sliding is observed experimentally is $v_c\sim1$ μm/s$=10^{-9}$ nu. [4].

Equations of motion. We use Langevin equations for all mobile atoms, i.e., atoms that do not belong to a rigid substrate,

$$m_\alpha\ddot{r}_{i\alpha}=f_{i\alpha}^{(\rm int)}+\sum_{S=1}^{2}f_{i\alpha,S}, \tag{2}$$

where $r_{i\alpha}\equiv\{x_{i\alpha},y_{i\alpha},z_{i\alpha}\}$ is the coordinate of the *i*th atom and $\alpha=$ s or $\alpha=$ l for ''substrate'' or ''lubricant'' atoms, respectively.

The force $f^{(\mathrm{int})}$ is due to interaction between the mobile atoms in the system,

$$f_{i\alpha}^{(\mathrm{int})} = -\frac{\partial}{\partial r_{i\alpha}} \sum_{i'\alpha'}^{\mathrm{all}} V_{\alpha'\alpha}(r_{i'\alpha'} - r_{i\alpha}), \tag{3}$$

where the sum includes all ''mobile'' s and l atoms except the given (αth) one.

The last term in Eq. (2) describes the interaction of a ''mobile'' s- or l-atom with the bottom ($S=1$) and top ($S=2$) substrates. The force $f_{i\alpha,S}$ itself consists of three contributions as usual in Langevin equations,

$$f_{i\alpha,S} = f_{i\alpha,S}^{(\mathrm{int})} + f_{i\alpha,S}^{(\mathrm{fric})} + f_{i\alpha,S}^{(\mathrm{ran})}. \tag{4}$$

The first contribution $f_{i\alpha,S}^{(\mathrm{int})}$ comes from the potential interaction of a given ith atom with all ''immobile'' atoms of the Sth (bottom or top) rigid substrate,

$$f_{i\alpha,S}^{(\mathrm{int})} = -\frac{\partial}{\partial r_{i\alpha}} \sum_{i'=1}^{N_S} V_{s\alpha}(R_{i'S} - r_{i\alpha}), \tag{5}$$

where the sum now includes all ''immobile'' s atoms of the corresponding substrate and R_{iS} is the coordinate of the ith atom of the Sth rigid substrate.

The second and third contributions in Eq. (4) describe the energy exchange between mobile atoms and the rigid substrates. They approximately take into account the missing degrees of freedom of the substrates. More precisely, the second contribution $f_{i\alpha,S}^{(\mathrm{fric})}$ describes a viscous damping when an atom moves relative the corresponding substrate,

$$f_{i\alpha,S}^{(\mathrm{fric})} = -m_\alpha \eta(\ldots)(\dot{r}_{i\alpha} - \dot{R}_S), \tag{6}$$

where $\eta(\ldots)$ is the ''external'' damping coefficient that depends on the velocity and distance relative to the substrate,

$$\eta(\ldots) = \eta(z_{\mathrm{rel}}, v_{\mathrm{rel}}), \quad z_{\mathrm{rel}} = (-1)^{(S-1)}(z_{i\alpha} - Z_S),$$

$$v_{\mathrm{rel}} = \dot{r}_{i\alpha} - \dot{R}_S, \tag{7}$$

where $R_S \equiv \{X_S, Y_S, Z_S\}$ is the center-of-mass coordinate of the Sth substrate (for the bottom substrate we took $R_1 \equiv 0$). Finally, the third contribution $f_{i\alpha,S}^{(\mathrm{ran})}$ in Eq. (4) describes the random (Gaussian) force acting on the ith atom from the Sth substrate. The amplitude of this force is determined by the substrate temperature T, i.e., the corresponding correlation function is

$$\langle f_{i\alpha,S}^{(\mathrm{ran})}(t) f_{i'\alpha',S'}^{(\mathrm{ran})}(t') \rangle = 2\eta_R(\ldots) m_\alpha k_B T \delta_{ii'} \delta_{\alpha\alpha'} \delta_{SS'} \delta(t-t'). \tag{8}$$

The function $\eta_R(z_{\mathrm{rel}})$ in Eq. (8) coincides with the external damping coefficient $\eta(z_{\mathrm{rel}})$ if the latter does not depend on the velocity (but may depend on the coordinate). Otherwise, if the external damping depends on v_{rel}, the two coefficients are coupled by the relationship [27,28]

$$\eta_R(z,v,T) = \int_0^\infty d\epsilon\, e^{-\epsilon} \eta[z, \tilde{v}(\epsilon)], \quad \tilde{v}^2(\epsilon) = v^2 + \frac{2k_B T}{m_\alpha}\epsilon. \tag{9}$$

For the top rigid substrate we use Newton's equation of motion,

$$M_S \ddot{R}_2 = N_S f_{\mathrm{ext}} + F_S, \tag{10}$$

where $M_S = N_S m_S$ is the mass of the rigid substrate, $f_{\mathrm{ext}} = \{f, 0, f_{\mathrm{load}}\}$ is the external force applied to it, and $F_S = -\Sigma_{i\alpha}^{\mathrm{all}} f_{i\alpha,S=2}$ according to Newton's third law (conservation of the total momentum of the system). As we checked numerically, this technique leads to Gaussian distribution of velocities for all atoms as well as for the top rigid substrate with a correct width for a given temperature T.

External friction coefficient. Fortunately, the motion of a single atom or a submonolayer film adsorbed on a crystal surface, namely, their vibration near the equilibrium position, has been well studied experimentally and theoretically [29,30]. This allows us to model the external damping of lubricant atoms near the substrates with a reasonable accuracy. For the external damping coefficient $\eta(z,v)$, which models the energy loss of an atom into the substrates and enters into Eqs. (6–8), we take into account its dependence on the distance z from the corresponding substrate and on the relative velocity v according to $\eta(z,v) = \eta_1(z)\eta_2(v)$. First, we assume that the damping rate exponentially decreases when an atom moves away from the substrate, and saturates at some level when the atom approaches very close to the substrate,

$$\eta_1(z) = 1 - \tanh[(z - z^*)/z^*]. \tag{11}$$

The characteristic distance z^* is chosen as the height of the pyramid with the base constructed of four rigid substrate atoms with square length $a_s = 3$, and the vertex with the s atom at the distance $r_{ss} = 3$ from the rigid-substrate atoms; this leads to $z^* = 2.12$. Thus, for the atoms in the s layer, where $z \sim z^*$, we have $\eta_1 \sim 1$, while for the atoms in the first (closest to the substrate) lubricant layer we obtain $\eta_1 \sim 0.1$.

Second, to determine $\eta_2(v)$, we used the results known for the damping of the vibrations of an atom adsorbed on the crystal surface. According to the theory [30,31], when an atom vibrates with a frequency ω near its equilibrium position, the oscillation decays due to creation of phonons in the substrate with the rate

$$\eta_{\mathrm{ph}}(\omega) = \frac{\pi}{2}\frac{m_\alpha}{m_S}\omega^2 \rho(\omega), \tag{12}$$

where the surface local density of phonon states may be described approximately by the function [31]

$$\rho(\omega) = \frac{32}{\pi}\frac{\omega^2(\omega_m^2 - \omega^2)^{3/2}}{\omega_m^6}, \tag{13}$$

and ω_m is the maximum (Debye) phonon frequency of the solid substrate. The one-phonon damping mechanism works

for frequencies $\omega<\omega_m$. At higher frequencies the damping is due to multiphonon processes. Moreover, in the case of metal or semiconductor substrates there is an additional damping due to the creation of electron-hole pairs in the substrate so that the corresponding damping coefficient is typically of order $\eta\sim 10^{-2}\omega_m$ (see Refs. [30,31]). Using these results, we took for the dependence $\eta_2(v)$ the following approximate expression:

$$\eta_2(v)=\eta_{\min}+\eta_{\rm ph}(2\pi v/a), \tag{14}$$

with $a=a_s$ for the motion along the substrate and $a=z^*$ for the motion in the z direction. For the minimal contribution $\eta_{\min}$ we chose $\eta_{\min}=0.01$ and $\omega_s=0.049$. This value is compatible with the justifications given above, and it leads to a thermalization of the system in reasonable simulation times $t<3\times 10^3\tau_s$. The cutoff (Debye) frequency was found from the phonon spectrum (the Fourier transform of velocities of all atoms and the top rigid substrate calculated for $f=0$ at $T=0.025$) which gives $\omega_m=15$. Thus, as a function of frequency the external damping behaves as

$$\eta_2(\omega)=\eta_{\min}+16\,\omega_m\left(\frac{\omega}{\omega_m}\right)^4\left[1-\left(\frac{\omega}{\omega_m}\right)^2\right]^{3/2}, \tag{15}$$

so that at small frequencies, $\omega\ll\omega_m$, we have $\eta_2(\omega)\approx\eta_{\min}+(16/\omega_m^3)\,\omega^4\approx(4.9+0.47\,\omega^4)\times 10^{-2}$, while at the frequency $\omega=(4/7)^{1/2}\omega_m=11.34$ the external damping reaches its maximum value $\eta_2\approx 22$.

Energy losses. When one part of a system moves with respect to another part with a relative velocity v, then the rate at which work is done is equal to $\varepsilon=vf$, where f is the total force acting on the former. This may be used to define the energy losses of a given atom as

$$\varepsilon_i=-\frac{1}{2}\sum_{i'}(v_i-v_{i'})f_{ii'}, \tag{16}$$

where the sum is over *all* atoms of the system including the s atoms of the rigid substrates, and $f_{ii'}$ is the force acting on the i'th atoms from the i'th one. Note that this force has to include the damping and random (Gaussian) contributions of the total force when i' corresponds to the s atom of rigid substrates. Then, taking a corresponding sum over atoms and averaging over time, one can find the energy losses in a given atomic layer of the lubricant, or those in the substrates, as well as separate contributions from different degrees of freedom.

To illustrate this definition, let us consider an ideal case in which the bottom substrate is immobile, the top substrate moves with a velocity v in the x direction, and the lubricant film with the velocity $\frac{1}{2}v$ while the force F is applied to the top substrate. We have $F_{\rm lub/top}=-F_{\rm top/lub}=F_{\rm bot/lub}=-F_{\rm lub/bot}=F$, and we obtain $\varepsilon_{\rm top}=-\frac{1}{2}(-F)(v-\frac{1}{2}v)=\frac{1}{4}Fv$, $\varepsilon_{\rm lub}=-\frac{1}{2}[F(\frac{1}{2}v-v)-F\frac{1}{2}v]=\frac{1}{2}Fv$, and $\varepsilon_{\rm bot}=-\frac{1}{2}F(0-\frac{1}{2}v)=\frac{1}{4}Fv$, thus the total losses are equal to $\varepsilon=Fv$, which coincides with the work done by the external force as expected.

Curved substrates. In most simulations both top and bottom substrates were flat. However, we have done also a few runs with curved substrates [32], where the z coordinate of the bottom rigid substrate is defined by

$$z=-\frac{1}{2}h_x^{(\rm dn)}r_{sl}\left(1-\cos\frac{2\pi x}{L_x}\right)-\frac{1}{2}h_y^{(\rm dn)}r_{sl}\left(1-\cos\frac{2\pi y}{L_y}\right), \tag{17}$$

where $L_{x,y}$ is the size of the system in the x or y direction and $h_{x,y}$ are the corresponding curvature parameters. Similarly the z coordinate of the top rigid substrate is defined by the expression

$$z=Z_2+\frac{1}{2}h_x^{(\rm up)}r_{sl}\left[1-\cos\frac{2\pi(x-X_2)}{L_x}\right]+\frac{1}{2}h_y^{(\rm up)}r_{sl}\left[1-\cos\frac{2\pi(y-Y_2)}{L_y}\right], \tag{18}$$

where $\{X_2,\ Y_2,\ Z_2\}$ are the center-of-mass coordinates of the top rigid substrate.

Algorithm. In most of the simulations we used the constant-force algorithm [21,22]. Namely, at the beginning we equilibrate the system at a temperature T (in this paper we present the results for $T=0$ and $T=0.025$, which corresponds to room temperature for energies measured in eV). Then we adiabatically increase the shear force f in steps Δf (typically $\Delta f=10^{-3}$ or smaller). Each increase of f is accomplished progressively in i_t (typically $i_t=200$ or more) substeps each of duration τ_s. When f has reached its new value, we wait during a time $i_t\tau_s$ in order to allow the system to reach a stationary state, and then measure the atomic coordinates and velocities during the next time interval $i_t\tau_s$. Thus, the force is changing with the average rate $\mathcal{R}/3\tau_s$, where $\mathcal{R}=\Delta f/i_t$. In some simulations we also used the constant-velocity algorithm (which is typically used in tribology simulations, see Ref. [9]), when a constraint is used to keep constant the top substrate velocity. We found, however, that the const-v algorithm leads to a much smaller accuracy of the results than the const-f one, probably because the friction force in this case is not a self-averaging value. Thus, here we present the results of the const-f runs only.

Most of the simulations have been done for a rather small system. The issue of system size raises the usual question in computer simulations of whether it is better to take a small system and study it carefully or to take a larger system and do a less comprehensive study over shorter times. Our simulations show that the processes under investigation are characterized by long relaxation times. The approach with adiabatic changing of the driving force necessitates going through a whole cycle of f changes. For a much larger system it is not possible to reach equilibrium in a reasonable time for this type of study. However, we also made a few runs for a system four times larger and found that the results did not change. Besides, in physical systems microscopic contacts are of a size similar to that of our system, for example 10×10 atoms. Even in specially prepared surfaces, with experiments performed in high-vacuum conditions,

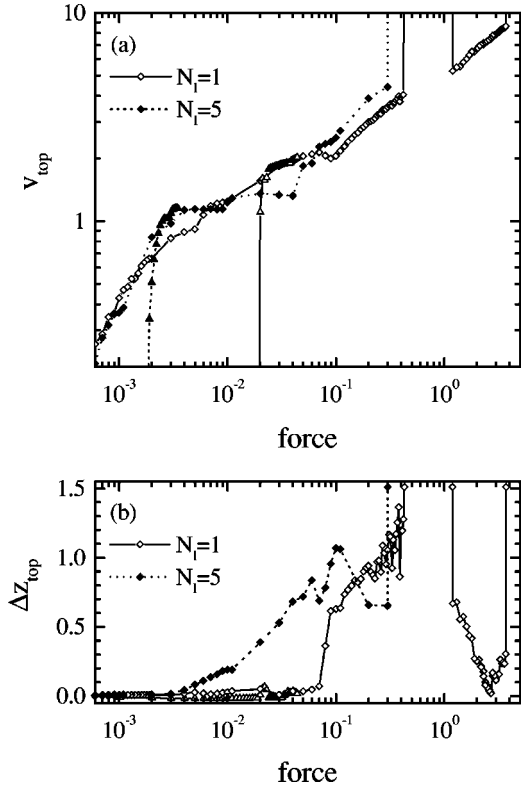

FIG. 2. (a) The velocity of the top substrate and (b) the change of the lubricant thickness for the one-layer (solid curves and open diamonds) and five-layer (dotted curves and solid diamonds) lubricant films.

ideal surfaces usually do not extend beyond about 30 lattice constants. Of course the results deduced from such simulations of ideal surfaces should not be used without extreme caution to analyze the results of macroscopic experiments. We shall come back to this point in the discussion because the connection with macroscopic experiments is a difficult point for all studies of microscopic friction, whether they are experimental (with atomic force microscope) or numerical.

III. RESULTS

Before going into the details of simulation results, let us discuss some general features. Typical dependencies of the velocity of the top substrate in the x direction, $v_{\mathrm{top}}(f)$, and the change of its z coordinate, $\Delta z_{\mathrm{top}}(f)$, as functions of the driving force f for the one- and five-layer lubricant films are shown in Fig. 2. Each plotted point is the average over $i_t = 200$ data points recorded at times separated by $\Delta t = \tau_s$ and corresponds to the steady-state motion for a given f. Let us analyze first the behavior of the five-layer film. The motion starts when the force exceeds a static friction force $f_s \approx 0.0017 - 0.0018$. One can see a plateau on the $v_{\mathrm{top}}(f)$ dependence for the force interval $2\times10^{-3} < f < 0.03$, then at larger forces v_{top} approximately linearly increases with f, and finally at $f \geqslant f_f \approx 0.30 - 0.31$ the ''regular'' motion is destroyed. The velocity of the top substrate for these force intervals lies within the interval $1 < v_{\mathrm{top}} < 4.5$, so that the washboard frequency, defined as $\omega_{\mathrm{wash}} = \pi\langle v_{\mathrm{top}}\rangle/a$, lies just

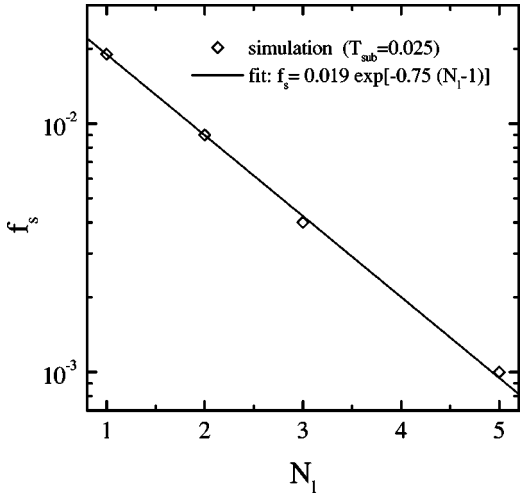

FIG. 3. The static friction force f_s as function of the number of lubricant layers N_l for $T = 0.025$.

inside the phonon spectrum of the lubricant film as will be discussed in details later. In this force range, the width z of the film increases as shown on Fig. 2(b). The system exhibits hysteresis: if one starts with a force $f < f_f$ and then decreases it adiabatically slowly, the system comes back to the $T = 0$ ground state for a force $f_b \approx 2\times10^{-5}$, which is much lower than f_s. The velocity of the top substrate at the backward transition drops down abruptly from a value $v_b \approx 0.03$ to zero. Moreover, if we start from the sliding state and then remove the driving force at all, the system again comes to the $T = 0$ ground state.

The behavior of thinner lubricant films is very similar. For example, the one-layer film starts to move at $f_s \approx 0.019 - 0.02$. The forward transition now takes place at $f_f \approx 0.43$, which is slightly larger than that for the five-layer film, although the velocity at which the film starts to melt is approximately the same, $v_f \approx 4$. The backward transition takes place at $f_b \approx 1.5\times10^{-4}$ when $v_b \approx 0.085$.

Although the sliding regime is approximately the same for different lubricant widths, the static frictional force needed to initiate the sliding, decreases approximately exponentially as the width increases as shown in Fig. 3. The dependence $f_s(N_l)$ may be explained qualitatively in the following way. To initiate the sliding the lubricant atoms must overcome barriers created by the substrate atoms. But the height of the barriers strongly (exponentially) depends on the distance z of the lubricant atoms from the substrate. It decreases when the lubricant atoms are moved away from the substrate. In the one-layer case the confined lubricant has to adjust to both substrates simultaneously and thus has no freedom to move in the z direction. On the other hand, when the lubricant is thicker, its utmost layers can move in the z direction due to elasticity of the film, and thus can allow the atomic positions to find a minimum-energy saddle configuration. This is confirmed by the analysis of the system configurations just before f_s. They show that the shifts of the atoms in the z direction from their $f = 0$ equilibrium positions in the five-layer film are much larger than those in the three-layer film, which in turn are larger than in the two-layer film.

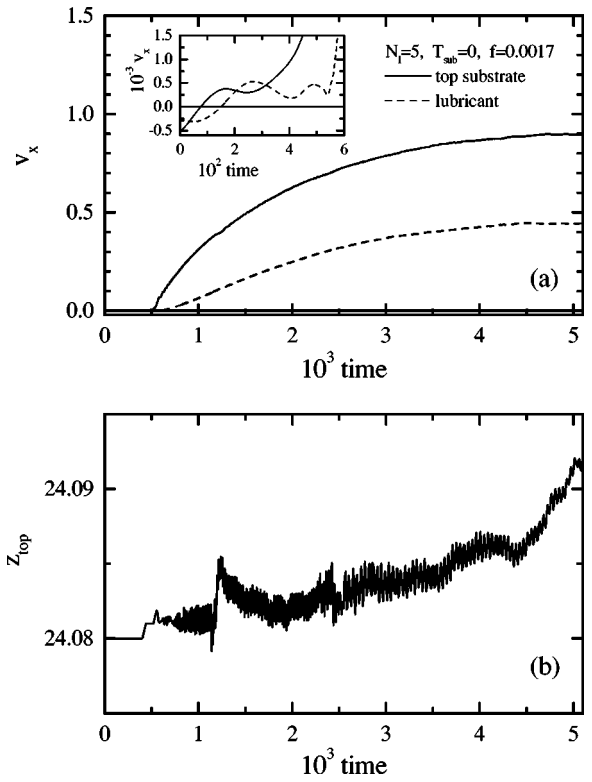

FIG. 4. Beginning of the sliding of the five-layer film. (a) The x velocity of the top substrate (solid curve) and the lubricant (dashed curve). Inset: the same enlarged for shorter times. (b) z_{top} versus time.

The dependence of the static force f_s on the temperature T is only significant for $N_l>1$ when the lubricant atoms have enough freedom to move in the z direction. For example, for the five-layer film we found $f_s\approx 0.0017$ at $T=0$ but $f_s \approx 0.001$ at $T=0.025$.

The initial stage of the sliding is illustrated on Fig. 4, where we plot $v_x(t)$ for the top substrate and the lubricant and $z_{\mathrm{top}}(t)$ for the five-layer film. One can see that at the beginning, the top substrate (the rigid substrate with one attached s layer) starts to move first. Its velocity increases according to a law $v_{\mathrm{top}}(t)\approx[f_s/(m_s+m_S)\,\eta_{\mathrm{eff}}(t)][1-\exp -\eta_{\mathrm{eff}}(t)(t-t_s)]$, where the effective friction coefficient is defined as $\eta_{\mathrm{eff}}=f/(m_s+m_S)v_{\mathrm{top}}$, and achieves a plateau in the steady state. Soon after, however, the lubricant is also involved into the motion and reaches the velocity $v_{\mathrm{lub}} =\frac{1}{2}v_{\mathrm{top}}(f_s)$ in the steady state. Simultaneously, the width of the lubricant slightly increases. We observed that for our system sizes, the lubricant begins to move as a whole. All its atoms begin to move almost simultaneously. However, for larger sizes of the contact one could expect that the sliding may begin with the creation of ''moving islands'' [33].

An interesting result is that the one-layer film can be in the sliding steady state for much larger dc forces than thicker films. The solid sliding exists for forces within the interval $1.1<f<3.7$ when the velocity is $5<v_{\mathrm{top}}<9$. This steady state cannot be reached by adiabatically increasing the force because the lubricant melts earlier. But it can be obtained with a sharp increase of the force, e.g., if one takes the $f=0.2$ steady state and applies the force $f=2$. This high-speed steady state corresponds to the ''flying'' regime predicted in Ref. [22] and will be described in more detail below in Sec. IV.

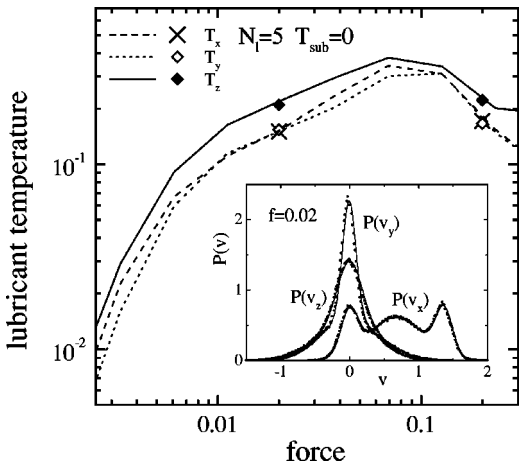

FIG. 5. Lubricant temperatures versus force for a five-layer film. Inset: velocity histograms (dots) and the corresponding Gaussian distributions (solid curves) for $f=0.02$.

A. Solid sliding

All steady states described above correspond to a solid sliding regime, in which the lubricant moves as a whole with a velocity equal to half of the velocity of top substrate. The distributions of velocities for all forces can be well approximated by Gaussian curves if we use different ''temperatures'' for the lubricant and the s-atomic substrate layers as well as for different degrees of freedom. For example, for the five-layer film we show in the inset of Fig. 5 the velocity histograms for the $f=0.02$ case by dotted curves and the corresponding Gaussians by solid curves. Thus, we can define the ''temperature'' for a given degree of freedom ($\alpha =x,y,z$) as well as for a given layer l of the lubricant or the substrate as $T_\alpha=m\langle(v_\alpha-\langle v_\alpha\rangle)^2\rangle$, where $\langle\ldots\rangle$ designates the averaging over time and over all atoms in the given layer, and then use the values $T_\alpha(l)$ (let $l=0$ corresponds to the s-atomic layers of the bottom substrate, $l=1$ corresponds to the first layer of the lubricant film, etc.) as reliable characteristics of the driven system. The distribution of temperatures across the system is shown in Fig. 6(a). First, note that compared with the lubricant temperatures, the temperatures of s layers of the substrates are very small (for the $T=0$ simulation). Second, at low force velocities the temperature is not uniformly distributed over the lubricant film; the boundary layers that are in moving contact with the substrates have a higher temperature than those in the middle of the lubricant. But at high forces velocities, $f\sim 0.02-0.2$ when $v_{\mathrm{top}}\sim 1-4$, the lubricant temperature is approximately uniform across the lubricant. This indicates that anharmonicity effects, which are responsible for energy exchange between different layers within the lubricant, become large enough at these forces. Third, the lubricant temperature increases with growing f (see Fig. 5) until it finally melts at

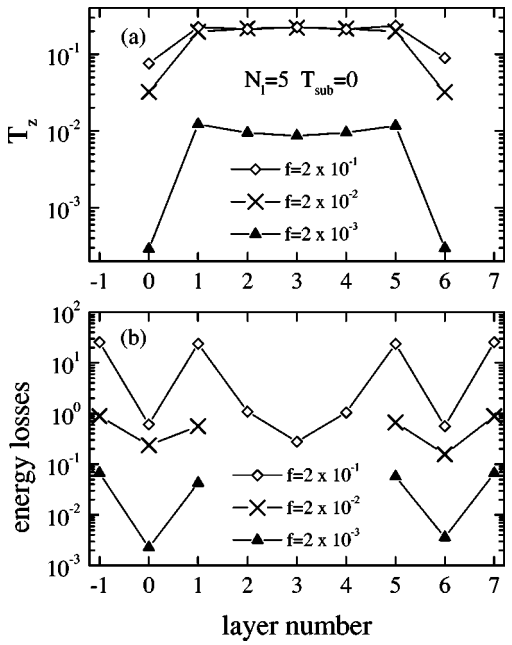

FIG. 6. Distribution of (a) the temperature T_z and (b) the energy losses across the five-layer lubricant for different dc forces f at $T_{\rm sub}=0$. The numbers -1 and 7 correspond to the rigid substrates, the numbers 0 and 6 correspond to the *s*-atomic substrate layers, and the numbers 1 to 5 correspond to the lubricant layers.

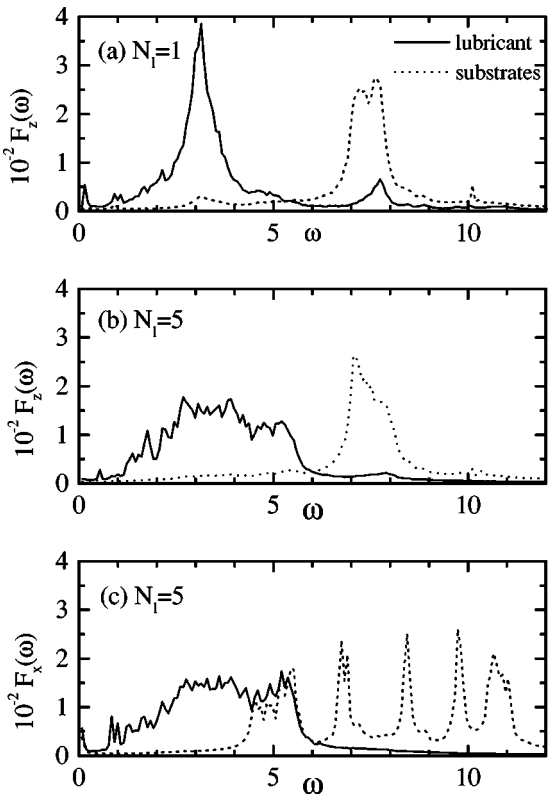

FIG. 7. Phonon spectra of the lubricant (solid curves) and the substrates (dotted curves) for one- and five-layer films.

$f=f_f$. Fourth, for all studied cases we found that $T_z \gg T_x \gtrsim T_y$. This indicates that the driven system is strongly out of equilibrium.

The calculation of energy losses $E_{\rm loss}$ for different dc forces shows that total losses are close to the expected values. For example, for $f=0.002$ we obtained $E_{\rm loss}\approx 0.24$, while $fv_{\rm top}\approx 0.26$; for $f=0.02$, $E_{\rm loss}\approx 3.2$ ($fv_{\rm top}\approx 3.6$), and for $f=0.2$, $E_{\rm loss}\approx 102$ ($fv_{\rm top}\approx 103$) correspondingly. The energy is lost mainly due to the motion of atoms along the direction x of the driving, the y and z components of the losses are negligible. The distribution of energy losses in the normal direction of the system is shown in Fig. 6(b). One can see that the energy is lost mainly within the rigid substrates and in the utmost lubricant layers (i.e., in the layers that are in moving contact with the substrates).

To analyze in detail the energy losses for the solid-sliding regime, we have to know the phonon spectrum of the system. To find it, we saved the coordinates of all atoms at $f=0$ and temperature $T=0.025$, and then calculated the Fourier transform

$$F_\alpha(\omega)=\sum_j \left| \int dt\, v_{j\alpha}(t) e^{i\omega t} \right|, \tag{19}$$

where the sum may be over all atoms or only over a selected subset, such as the lubricant atoms. The spectra calculated in this way for different degrees of freedom ($\alpha=x,y,z$) separately for the substrates and the lubricant are shown in Fig. 7 for $N_l=1$ and 5. One can see that the lubricant spectrum occupies the frequencies $1\lesssim\omega\lesssim 6$, while the substrate modes lie mainly within the interval $6<\omega<\omega_m$. The x and y spectra are broader than the z spectrum. For the one-layer lubricant, the spectrum $F_z(\omega)$ for the lubricant has a maximum at $\omega\sim 3$, which is quite sharp.

Calculating in the same manner the spectrum in the solid-sliding regime, we observed the excitation of z oscillations of the lubricant with the frequency $\omega=\omega_{\rm wash}$ as indicated by arrows in Fig. 8. We also found that (a) the intrinsic energy losses in the lubricant become important only when $\omega_{\rm wash}$ is higher than the lower boundary of the lubricant phonon spectrum, $\omega_{\rm wash}\gtrsim 1$; (b) at $f=2\times 10^{-3}$ one can see many higher-frequency harmonics of $\omega_{\rm wash}$, i.e., the vibration of lubricant is highly anharmonic; when the force increases even more, the energy exchange between the modes of the lubricant distributes the energy among all the lubricant modes; and (c) at $f=0.02$ and $f=0.2$ the lubricant is strongly heated and the energy of the translational motion is distributed over all three (x, y, and z) degrees of freedom.

The behavior of the thin $N_l=1$ film is similar. The temperatures of the lubricant begin to increase at $f>4\times 10^{-3}$ when the velocity is $v_{\rm top}>1$ so that the washboard frequency penetrates into the lubricant phonon spectrum. Then at $f\gtrsim 0.1$ the excitation of lubricant vibrations strongly increases, especially for the z coordinate, so that the width of the film begins to increase [see Fig. 2(b)]. The temperature reaches the value $T_z\sim 0.4$, and soon the lubricant melts. On the other hand, for the high-force sliding state (the ''flying'' regime) the perturbation of the film is much smaller, $\Delta z<0.5$ and $T_z\sim 0.1$. At small forces velocities the energy losses are mainly in the rigid substrates. At $f\sim 0.02-0.2$ the

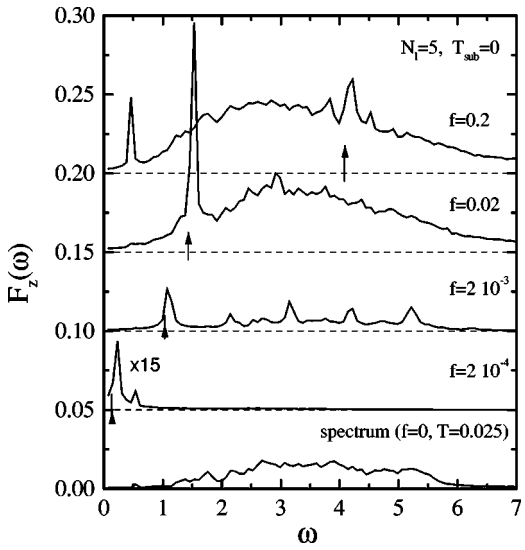

FIG. 8. Change of the z spectrum (19) of a five-layer lubricant with increasing driving force. The arrows indicate the position of the washboard frequency. The curves for $f\neq 0$ are artificially shifted upstair.

losses are approximately equally distributed between the two rigid substrates and the lubricant. Finally, in the high-force ''flying'' regime the main losses are in the lubricant film.

B. Effective friction coefficient

In a steady-sliding regime, where the top rigid substrate and one s layer attached to it slide over the lubricant film, it is convenient to introduce the effective friction coefficient as

$$\eta_{\rm eff}(v_{\rm top})=\frac{f}{(m_S+m_s)v_{\rm top}(f)}. \tag{20}$$

Note that a change of the velocity of the top substrate can be expected to take a time of the order $\tau_{\rm relax}=\eta_{\rm eff}^{-1}$. Using the results of simulations, one can see that at small forces the effective friction can be smaller than $\eta_{\rm eff}<10^{-3}$, so the relaxation times are larger than $\tau_{\rm relax}>10^3$.

Energy loss can only occur through the externally imposed damping. One part comes from the motion of the lubricant as a whole. This is the loss that one would get if the lubricant were sliding as a perfect solid relative to the rigid substrates. The corresponding contribution to the effective friction coefficient is due to the external damping [with the coefficient $\eta(z,v)$ introduced into the equations of motion from the beginning] of the uniform x motion of lubricant atoms relative the substrates with the velocity $\frac{1}{2}v_{\rm top}$, and yields a ''universal'' dependence $v_{\rm top}^{\rm (uni)}(f)$ which does not depend either on the lubricant width or on the masses m_s and m_S. In what follows we call this contribution as the ''perfect-sliding'' one. A second part comes from the internal motions inside the lubricant and the surface layers of the substrates. The driving excites atomic vibrations (mainly in the z direction as mentioned above) which then are distributed over other (x and y) degrees of freedom and finally are damped again due to the external damping $\eta(z,v)$. This contribution will be called below as the ''internal-losses'' one.

In the solid-sliding regime, when the top rigid substrate with one attached s layer moves as a whole with a velocity $\langle v_{\rm top}\rangle$, the bottom rigid substrate with one attached s layer does not move at all, and the lubricant film moves as a whole with the velocity $v_{\rm lub}=\frac{1}{2}\langle v_{\rm top}\rangle$, the washboard frequency is equal to

$$\omega_{\rm wash}=2\pi v_{\rm lub}/a=\pi\langle v_{\rm top}\rangle/a, \tag{21}$$

where one should take $a=a_s=3$. Let us write the balance of forces for the top substrate with one attached s layer as

$$F\equiv N_S f=N_{al}m_l\eta^*(v_{\rm top})\,v_{\rm lub}, \tag{22}$$

where we have introduced the total viscous damping coefficient $\eta^*(v_{\rm top})$ for an atom in the utmost lubricant layer. Using the definition (20) of the effective friction coefficient, we obtain the following relationship between the coefficients $\eta_{\rm eff}(v_{\rm top})$ and $\eta^*(v_{\rm top})$,

$$\eta_{\rm eff}(v_{\rm top})=\frac{1}{2}\,\frac{m_l}{m_S+m_s}\,\frac{N_{al}}{N_S}\,\eta^*(v_{\rm top}). \tag{23}$$

In a general case the total damping $\eta^*(v_{\rm top})$ defined by Eq. (22), has to consist of two contributions, the ''perfect-sliding'' contribution $\eta_{\rm ext}(v_{\rm top})$ and the intrinsic losses $\eta_{\rm int}(v_{\rm top})$. In the two following subsection we evaluate successively these two components of the losses.

1. ''Perfect-sliding'' contribution to the energy loss

In the perfect-sliding approximation the atoms in the utmost lubricant layers feel only the external damping $\eta_{\rm ext}(v_{\rm top})\approx\eta_1(z_{\rm lubr})\,\eta_2(\omega_{\rm wash})$ due to energy exchange with the rigid substrates. Substituting the washboard frequency (21) into Eq. (15), we obtain

$$\eta_{\rm ext}(v_{\rm top})\approx\left[1-\tanh\left(\frac{z_{\rm lubr}-z^*}{z^*}\right)\right]\times\left[\eta_{\rm min}+\frac{16\pi^4}{a_s^4\omega_m^3}v_{\rm top}^4\left(1-\frac{\pi^2}{a_s^2\omega_m^2}v_{\rm top}^2\right)^{3/2}\right]. \tag{24}$$

Assuming that all the damping within the lubricant is due to the external one, $\eta^*(v_{\rm top})=\eta_{\rm ext}(v_{\rm top})$, we obtain the ''universal'' (''perfect-sliding'') dependence

$$v_{\rm top}^{\rm (uni)}(f)=\frac{2N_S}{N_{al}}\,\frac{f}{m_l\eta_{\rm ext}(v_{\rm top})}, \tag{25}$$

which does not depend on the number of lubricant layers or on the substrate masses m_s and m_S, because it corresponds to the steady state (while a delay of response of $v_{\rm top}$ when f varies nonadiabatically, has to depend on the masses).

In particular, for the parameters used in simulation ($m_l=m_s=m_S=1$, $N_S=132$, and $N_{al}=80$), we obtain $\eta_{\rm eff}=0.15\,\eta^*$. Then, using, in Eq. (24), the values $z^*=2.12$,

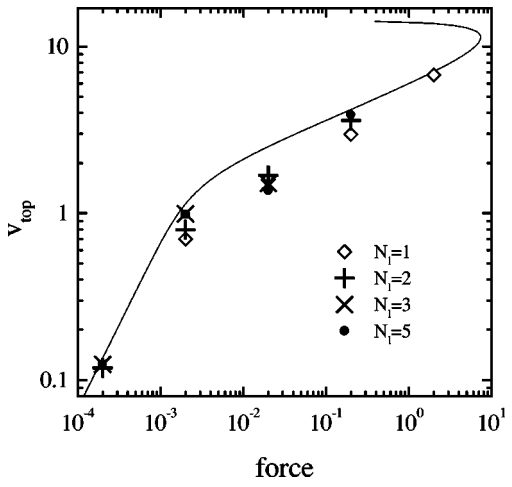

FIG. 9. The ''perfect-sliding'' dependence (25) and the $T=0$ simulation results.

$\omega_m=15$, and $a_s=3$, and taking from the simulation $z_{\rm lubr}\approx 5.25$ for the $T=0$ ground-state configuration, we obtain $\eta_{\rm ext}(v)\approx[4.9+0.57\,v^4(1-0.49\times10^{-2}v^2)^{3/2}]\times10^{-3}$, so that the external phonon damping exceeds the minimal one (which models the electron-hole damping) at $v_{\rm top}\gtrsim 1.7$ and reaches its maximum value $\eta_{\rm ext}\approx 2.16$ at $v_{\rm top}\approx 10.8$. If all the damping within the lubricant were due to the external one, the effective friction coefficient would be equal to

$$\eta_{\rm eff}^{\rm (uni)}(v_{\rm top})\approx 0.728\times10^{-3}\times[1+0.116\,v_{\rm top}^4(1-0.49\times10^{-2}v_{\rm top}^2)^{3/2}] \tag{26}$$

with the maximum $\eta_{\rm eff}\approx 0.32$. The ''perfect-sliding'' dependence (25) is presented in Fig. 9. One can see that it agrees rather well with the simulation data at small ($f<10^{-3}$) as well as at high ($f>1$) forces, when the washboard frequency lies outside the lubricant phonon spectrum and, thus, the internal motions of the lubricant are not excited.

An important result of this analysis is that the lubricant cannot support a force larger than $f_{\rm max}\approx 7$ when $v_{\rm top}\approx 10.8$. At larger forces velocities the system cannot dissipate the energy injected into it due to driving, and the solid-sliding regime must be destroyed.

However, in the simulation we found that $v_{\rm top}(f)<v_{\rm top}^{\rm (uni)}(f)$ and $f_f<f_{\rm max}$ in all cases. To describe simulation results more accurately, the following three factors have to be taken into account: (i) at velocities $v_{\rm top}>1-2$ the lubricant width increases (due to anharmonicity of the LJ potential), (ii) there are additional intrinsic energy losses within the lubricant as well as in the *s* layers, and (iii) due to these intrinsic energy losses, the lubricant is heated during the sliding. The first factor increases $v_{\rm top}$, while the second and third ones tend, on the contrary, to decrease it so that they must be studied in detail before a conclusion can be drawn.

2. Excitation of lubricant vibrations

When the lubricant film moves over the bottom substrate with the velocity $v_{\rm lub}$ dragged by the top substrate with the dc force $F=N_S f$, the dragging force per lubricant atom in the topmost lubricant layer is equal to $f_{\rm lub}=(N_S/N_{al})f$. The total energy injected into the lubricant by the external dc force per time unit per one lubricant atom is equal to

$$\varepsilon_{\rm tot}=f_{\rm lub}v_{\rm lub}=m_l\eta^* v_{\rm lub}^2, \tag{27}$$

where we used the definition (22) of the coefficient η^*. This energy must be absorbed in the system. One channel of energy dissipation, the energy exchange with the rigid substrates, was already considered in the previous section, and it yields

$$\varepsilon_{\rm ext}=m_l\eta_{\rm ext}v_{\rm lub}^2. \tag{28}$$

An extra energy losses, $\varepsilon_{\rm int}=\varepsilon_{\rm tot}-\varepsilon_{\rm ext}$, must be attributed to intrinsic losses within the system.

To study the intrinsic losses, we will use a technique similar to that described in Refs. [34,19,21]. Let us consider the internal vibrations of the system as a damped oscillator $\xi(t)$ of mass m, internal frequency ω_0, and damping coefficient η_0, where η_0 corresponds to the so-called full width at half maximum of the spectrum (a generalization to many oscillators is trivial). If the oscillator is excited by an external force oscillating with the frequency ω and the amplitude f_0,

$$m\ddot{\xi}+m\eta_0\dot{\xi}+m\omega_0^2\xi=f(t)={\rm Re}(f_0e^{i\omega t}), \tag{29}$$

the steady-state motion of the oscillator corresponds to its vibration with the frequency of the external oscillating force,

$$\xi(t)=\frac{f_0}{m}{\rm Re}\left(\frac{e^{i\omega t}}{\omega_0^2-\omega^2+i\omega\eta_0}\right). \tag{30}$$

The rate of energy losses (the energy absorbed by the oscillator per one time unit) is equal to

$$\varepsilon_{\rm osc}(\omega;\ \omega_0,\eta_0,f_0)=\frac{1}{\tau}\int_0^\tau dt\, f(t)\dot{\xi}(t)=\frac{1}{2}\omega\frac{f_0^2}{m}\rho(\omega), \tag{31}$$

where $\tau=2\pi/\omega$ and

$$\rho(\omega)={\rm Im}\left(\frac{1}{\omega_0^2-\omega^2+i\omega\eta_0}\right)=\frac{\omega\eta_0}{(\omega^2-\omega_0^2)^2+(\omega\eta_0)^2}. \tag{32}$$

In the solid-sliding regime the oscillating force is due to motion of the lubricant film over the corrugated substrates and thus is characterized by the frequency $\omega=\omega_{\rm wash}$. Then, assuming that the system can be described as k different oscillators and using Eqs. (27–32), we finally obtain $\eta^*(v_{\rm top})=\eta_{\rm ext}(v_{\rm top})+\eta_{\rm int}(v_{\rm top})$, where

$$\eta_{\rm int}(v_{\rm top})=m_l^{-1}(v_{\rm top}/2)^{-2}\sum_{i=1}^{k}\varepsilon_{\rm osc}(\omega_{\rm wash};\ \omega_0^{(i)},\eta_0^{(i)},f_0^{(i)}). \tag{33}$$

To fit the simulation data, we also assumed that the oscillator's damping coefficient depends on the frequency accord-

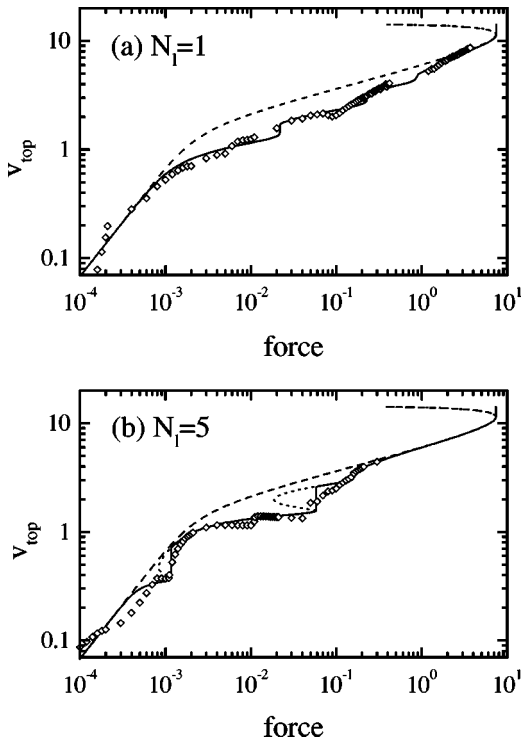

FIG. 10. Fitting of the simulation results for (a) $N_l=1$ and (b) $N_l=5$. Open diamonds are for the simulation data, the dashed curve shows the ''universal'' dependence (25), the dotted curve is obtained with Eqs. (31)–(33), and the solid curve is obtained from the dotted one by removing the unstable branches where $dv_{\rm top}(f)/df<0$. For the fitting we used the following frequencies, $\omega_0^{(1)}=7.3$, $\omega_0^{(2)}=5$, $\omega_0^{(3)}=3.3$, $\omega_0^{(4)}=1.65$, $\omega_0^{(5)}=0.4$, and the following fitting parameters for the widths of the resonance modes and the oscillating forces. (a) For $N_l=1$: $\tilde{\eta}_0^{(1)}=5$, $f_0^{(1)}=5$; $\tilde{\eta}_0^{(2)}=3$, $f_0^{(2)}=3$; $\tilde{\eta}_0^{(3)}=3$, $f_0^{(3)}=1.3$; $\tilde{\eta}_0^{(4)}=1.5$, $f_0^{(4)}=0.2$; $f_0^{(5)}=0$. (b) For $N_l=5$: $f_0^{(1)}=0$; $\tilde{\eta}_0^{(2)}=3$, $f_0^{(2)}=0.9$; $\tilde{\eta}_0^{(3)}=1$, $f_0^{(3)}=0.7$; $\tilde{\eta}_0^{(4)}=0.3$, $f_0^{(4)}=0.2$; $\tilde{\eta}_0^{(5)}=0.1$, and $f_0^{(5)}=0.006$.

ing to the expression $\eta_0^{(i)}(\omega)=\tilde{\eta}_0^{(i)}\eta_{\rm ph}(\omega)/\eta_{\rm ph}(\omega_0^{(i)})$, where $\tilde{\eta}_0^{(i)}$ is a constant. Then, from the spectra of Fig. 7 we choose the following five frequencies: $\omega_0^{(1)}=7.3$, which can be associated with the z vibrations of the substrates $\omega_0^{(2)}=5$, which describes the lowest x and y modes of the substrates, $\omega_0^{(3)}=3.3$, which corresponds to the lubricant oscillations, the frequency $\omega_0^{(4)}=\frac{1}{2}\omega_0^{(3)}$, which describes the excitation of the lubricant by the second harmonic of $\omega_{\rm wash}$, and finally (for the $N_l=5$ case only) $\omega_0^{(5)}=0.4$, which may be associated with the vibration of the top substrate as a whole. The results of fitting are presented in Fig. 10, where the values of the fitting parameters $\tilde{\eta}_0^{(i)}$ and $f_0^{(i)}$ are given in the caption to the figure. One can see that this simple approach gives a reasonable agreement with the simulation data and shows that the velocity of the top substrate is determined by the ''perfect-sliding'' approximation at forces $f<10^{-3}$, by the intrinsic losses corresponding to excitation of lubricant vibrations at forces $10^{-3}<f<0.1$, and by excitation of the substrate vibrations at higher forces. However, we have to

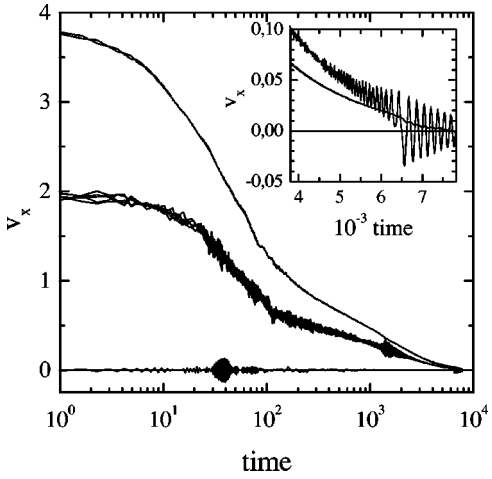

FIG. 11. The x velocities of the top substrate and all layers (including the s layers) versus time for the ''free'' run, when the five-layer system starts from the steady state corresponding to $f=0.2$ and then the driving force is removed. Inset: enlarged part of the dependencies at late times.

note that a general theory of kinetic friction, which could give, e.g., the values of the parameters $\tilde{\eta}_0^{(i)}$ and $f_0^{(i)}$ from first principles, is still lacking.

C. Minimal sliding velocity

As mentioned above, the system exhibits hysteresis: when the force decreases starting from the sliding state, a backward transition takes place at $f=f_b<f_s$, and the velocity drops down from a finite value $v_{\rm top}=v_b$ to zero. The same drop of the velocity is observed in free runs, when one starts with the solid-sliding steady state and then remove the driving: the velocity $v_{\rm top}$ slowly decreases till it reaches the minimal value v_b and then drops to zero as shown in Fig. 11. It is well known (e.g., see Ref. [35]) that a similar hysteresis is observed for a single driven particle at $T=0$. If a particle of mass M is placed into a sinusoidal external potential of (total) height $\mathcal{E}=\max V(x)-\min V(x)$ and period a, and is driven by the dc force F, the forward locked-to-running transition takes place at $F=F_s=\pi\mathcal{E}/a$, and the backward transition at $F=F_b=(2\sqrt{2}/\pi)\eta\sqrt{M\mathcal{E}}$, when the velocity is $\langle v_b\rangle\sim\sqrt{aF_s/M}$. In the underdamped case such that $\eta<\eta_c\equiv(\pi^2/2\sqrt{2})\sqrt{\mathcal{E}/Ma^2}$, we have $F_b<F_s$. Therefore the system exhibits hysteresis due to the inertia of the particle.

If the top substrate with the attached s layer would be treated as a rigid object, taking $a=3$ and $m_S+m_s=2$, the critical damping would be

$$\eta_c=\left[\frac{\pi^3}{8}\frac{f_s}{a(m_S+m_s)}\right]^{1/2}\approx 0.8\sqrt{f_s}. \tag{34}$$

The effective friction coefficient just above the transition to sliding is $\eta_s=f_s/(m_S+m_s)v_s$. Hysteresis is expected if $\eta_s<\eta_c$, i.e., $v_s>v_{bR}$, where

$$v_{bR}=\left(\frac{8}{\pi^3}\frac{af_s}{m_S+m_s}\right)^{1/2}\approx 0.62\sqrt{f_s}. \tag{35}$$

In the simulations the transition to sliding occurs for $f_s \sim 10^{-3}-10^{-2}$ while $v_s \sim 1$, so, for the chosen set of parameters, the system under investigation is clearly in the underdamped limit. We expect the backward transition at $f_b = (2\sqrt{2}/\pi\sqrt{\pi})\,\eta_{\rm eff}\sqrt{(m_S+m_s)\,a f_s} \approx 1.24\,\eta_{\rm eff}\sqrt{f_s}$.

Now we can check whether the condition $v_{bR} \approx 0.62\sqrt{f_s}$ agrees with the simulation data. For the solid-sliding regime with $V_{ll}=1$ at $T=0$, we found from free runs that for $N_l=1$, $f_s \approx (1.9-2)\times 10^{-2}$ and $v_b \lesssim 8.5\times 10^{-2}$, while $v_{bR} \approx 8.7\times 10^{-2}$; for $N_l=2$, $f_s \approx (8.9-9.1)\times 10^{-3}$ and $v_b \lesssim 6\times 10^{-2}$, while $v_{bR} \approx 5.9\times 10^{-2}$; for $N_l=3$, $f_s \approx (4-4.1)\times 10^{-3}$ and $v_b \lesssim 5\times 10^{-2}$, while $v_{bR} \approx 4\times 10^{-2}$; and for $N_l=5$, $f_s \approx (1.7-1.8)\times 10^{-3}$ and $v_b \lesssim 3\times 10^{-2}$, while $v_{bR} \approx 2.6\times 10^{-2}$. We also made runs for a smaller value of the interaction parameter $V_{ll}=1/3$, when the lubricant is weaker, and found that for $N_l=1$, $f_s \approx (1.3-1.4)\times 10^{-2}$ and $v_b \lesssim 8\times 10^{-2}$, while $v_{bR} \approx 7.2\times 10^{-2}$; and for $N_l=5$, $f_s \approx (1-1.1)\times 10^{-3}$ and $v_b \sim 1.5\times 10^{-2}$, while $v_{bR} \approx 2\times 10^{-2}$.

Thus, this simple inertia consideration quite well describes the hysteresis of the solid lubricant film and, at the same time, it shows that the minimal velocity of the top substrate in the solid-sliding regime cannot be smaller than $v_b \sim 10^{-2}$ nu$\sim$10 m/s, which is to be compared with the experimental value of the sliding to stick-slip transition $v_c \sim 10^{-6}$ m/s. This very large discrepancy will be discussed in Sec. IV. On the other hand, the friction $\mu = |f/f_{\rm load}|$ in the solid-sliding regime may be as small as $\mu \sim 10^{-4}-10^{-2}$.

Note that the value of v_b in Eq. (35) depends on the substrate mass m_S which, in principle, may be taken arbitrary large. However, in fact only one or few boundary layers of the substrate play a role, and the results presented above remains valid, at least qualitatively, for the infinite substrates as well [36,28].

D. Friction-induced melting

When the driving force approaches the threshold value $f=f_f$, the energy pumped into the lubricant due to sliding can no longer be removed from the contact region into the substrates, and the lubricant temperature strongly rises up to its melting temperature. The solid-sliding regime is destroyed. To study this process, we started from the $f=0.2$ steady-state configuration of the five-layer film, which is close to the threshold value $f_f \approx 0.31$, and applied the dc force $f=0.5$ to speed up the transition. The results are shown in Fig. 12. The velocity v_x of the top substrate grows approximately linearly with time. Because the top rigid substrate with one substrate layer attached to it moves as a whole during this process, we can use Newton's equation

$$(m_s+m_S)\dot{v}_\alpha = f_\alpha^{(\Sigma)} = f_\alpha^{(\rm intrinsic)} + f_\alpha^{(\rm external)}, \qquad (36)$$

which for the x coordinate takes the form $2\dot{v}_x = 0.5 - f_{\rm fric}$, where $f_{\rm fric}$ is the frictional force acting on the top substrate from the lubricant. One can see from Fig. 12(b) that $f_{\rm fric} \approx 0.3$ is the maximum force that lubricant losses can accommodate. Similarly one may find the normal force f_P acting on the top substrate from the lubricant, $2\dot{v}_z = f_{\rm load} + f_P$, which yields $f_P \approx 0.1$ (so that $f_{\rm load} + f_P \approx 0$) at the beginning,

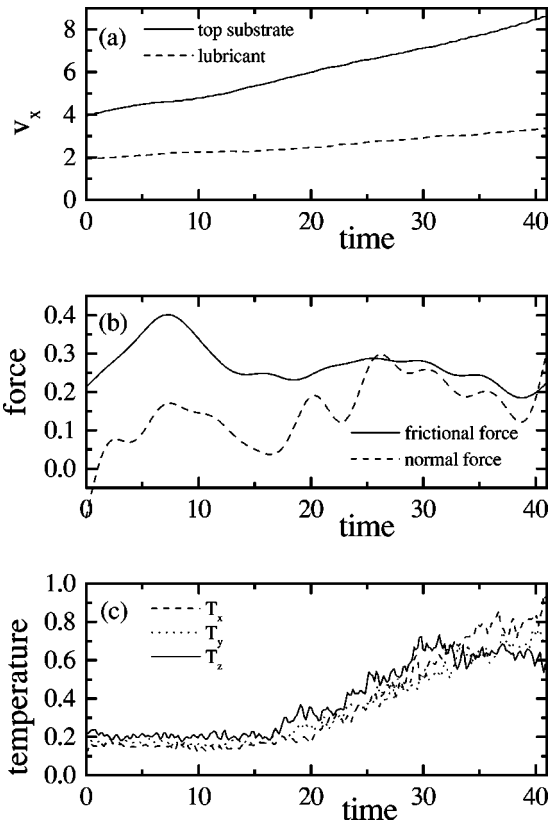

FIG. 12. ''Forced'' transition: the dependencies of (a) the x velocities of the top substrate and the lubricant, (b) the normal and frictional forces, and (c) the lubricant temperatures versus time, when the force $f=0.5$ is applied to an initial configuration corresponding to the $f=0.2$ steady state of the five-layer film at $T=0$.

but at $t>20$ the force f_P begins to grow and the width of the lubricant begins to increase. The lubricant temperature [see Fig. 12(c)] which was equal to $T_{\rm lub} \approx 0.2$ for the $f=0.2$ steady state, at $t>20$, begins to grow up to $T_{\rm lub} \sim 0.6-0.8$ which is much higher than the melting temperature $T_{\rm melt} \approx 0.4$, so the lubricant melts. Details of the forced transition are shown in Fig. 13, where we plot the z coordinates of all atoms in the system. For $t<20$ the lubricant slides as an ideal solid as it was for the $f=0.2$ steady state. At $t\sim 20$ the upper lubricant layers begin to slide over the lower layers, although the layers still keep the ideal triangular structure. At $t\sim 30$ the layers start to mix. At $t\sim 40$ the lubricant is already in the melted state, and the distribution of velocities across the lubricant $v(z)$ exhibits a gradient. After the melting, the lubricant cannot anymore support the applied dc force $f=0.5$ and $v_{\rm top} \to \infty$.

In another simulation we turned off the force at time $t=10.25$, when the lubricant was still in the solid-sliding state, and allowed the system to relax. This situation mimics that of real systems, where the driving force exists due to elastic stress within the substrates. Thus, when the relative velocities of the substrate and the lubricant sharply increase, the stress is relaxed and the driving force decreases (in principle this situation can easily be modeled with a spring attached to the top substrate [7]; unfortunately, one has to introduce simultaneously a few more model parameters). In

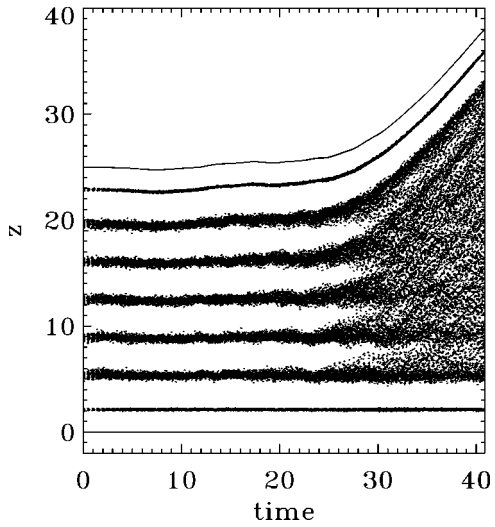

FIG. 13. The z coordinates of all atoms and the top rigid substrate during the ''forced'' transition shown in Fig. 12.

simulation we observed that although $f=0$ at $t>10.25$, the top substrate continues to slide owing to its inertia. During this sliding the lubricant again melts as one can see from Fig. 14. Then the lubricant temperature decreases, and the lubricant solidifies into a six-layer (amorphous) film at $t\gtrsim 300$ when $T_{\rm lub}\sim 0.3$, and finally stops (note that the final configuration obtained with this force-induced melting and then freezing, is similar to the configuration obtained by increasing the temperature until melting and then sharply decreasing it back to zero without the driving). The frictional force is large at the beginning when the lubricant melts ($f_{\rm fric}\sim 0.15$), but soon it quickly decreases to a value $f_{\rm fric}\sim 0.01$.

We also made similar experiments but with an applied force $f\neq 0$ ($f<0.5$) at time $t=10.25$. We observed that, if $f<0.005$, the system stops in a six-layer state. For $0.005<f<0.03$ we observed a sliding of the ''frozen'' six-layer lubricant; the lubricant temperature during the sliding is

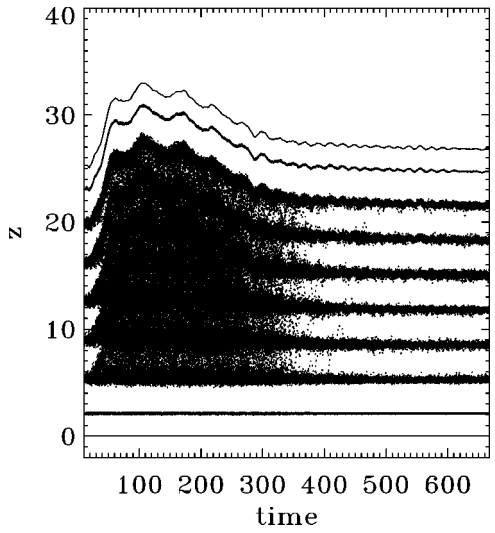

FIG. 14. The z coordinates of all atoms, when the driving force is removed at the time moment $t=10.25$ of the ''forced'' transition of Fig. 13.

$T_{\rm lub}\approx 0.06$ at $f=0.005$, $T_{\rm lub}\approx 0.14$ at $f=0.01$, and $T_{\rm lub}\approx 0.19$ at $f=0.02$. For $f=0.03$ we observed that $v\to\infty$, and the lubricant severs are in the middle. From the slope of the $v_{\rm top}(t)$ dependencies we found that $f_{\rm fric}\approx 0.028$, thus the frozen lubricant cannot support a driving force larger than $f\approx 0.03$.

Comparing the results obtained for a realistic external damping with the ones described above in the introduction, where the model with a constant damping coefficient was used, we see the essential difference. First, in the latter case the lubricant melts immediately when it begins to slide, i.e., $f_f<f_s$. This difference is due to the parameters chosen for the interatomic interaction. When the interaction of the lubricant with the substrates is much larger than the interaction within the lubricant, the scenario reviewed in the introduction is observed (the same also occurs if the lubricant is commensurate and perfectly aligned with the substrates). Second, after the shear-induced melting, the layer-over-layer sliding was observed, while now the transition to a ''gas'' phase takes place. Third, the back transition with force decrease now proceeds into an amorphous (frozen) state and not into the ideal solid one. These last two differences are due to a damping mechanism used in the simulation. As will be shown below in Sec. IV, when the model with a constant damping is used, the scenarios of the previous works are observed, which points out the importance of the damping mechanism on some results.

E. Sliding of curved substrates

The results presented above were obtained for ideally flat substrates. Due to periodic boundary conditions we have in fact infinite substrates and the lubricant atoms are strictly confined between them. In a real system, however, the lubricant may leave the contact region through open boundaries. Besides, the substrates may be not ideally flat. To study this situation, we made a few simulations for curved substrates for the $N_l=5$ system. The results are the following.

The $v_{\rm top}(f)$ dependence for the case when only one of the substrates (e.g., the top one) is curved in the x direction (along the driving direction) is presented in Fig. 15 by up triangles. In this case the lubricant film is approximately flat and follows the bottom (flat) substrate. At very low forces $f\leqslant 5\times 10^{-4}$, the lubricant moves together with the top substrate. For forces within the interval $5\times 10^{-4}<f<0.01$, the ideal solid-sliding regime exists. The lubricant film is approximately flat and slides over the flat bottom substrate, and the top substrate slides over the lubricant; in the contact region the lubricant is slightly compressed. For forces within the interval $10^{-3}<f<10^{-2}$ the velocity is approximately two times smaller than it was for the flat substrates. Note that because the real contact area takes now only half of the total surface, the real load pressure in the contact is two times larger. At higher forces, $f>10^{-2}$, the perturbation of the lubricant becomes significant. At $f\gtrsim 0.011$ some atoms from the topmost lubricant layer begin to escape into the empty space between the lubricant film and the curved top substrate, although they are pushed back when the bottom of the curved top substrate reaches them during the sliding. This

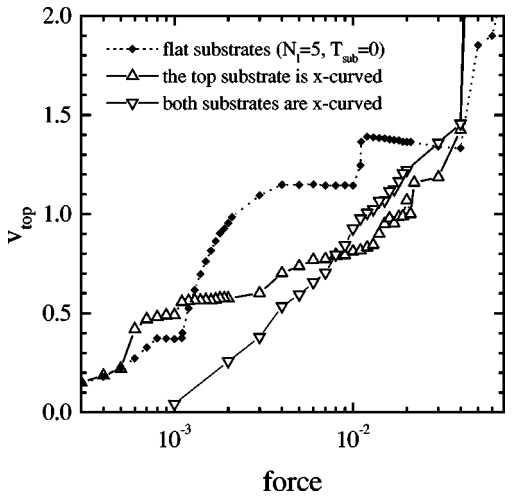

FIG. 15. The x velocity of the top substrate versus force for the five-layer lubricant film when the top rigid substrate is curved ($h_x^{(up)}=1$, $h_y^{(up)}=h_x^{(dn)}=h_y^{(dn)}=0$, the up triangles) and when both top and bottom rigid substrates are curved ($h_x^{(up)}=h_x^{(dn)}=0.5$, $h_y^{(up)}=h_y^{(dn)}=0$, the down triangles).

mixing increases with increasing of the dc force, and at $f \gtrsim 0.02$ the lubricant fills the empty space. In the thick part there are six layers. Finally at $f \approx 0.05$ (i.e., much earlier than for the flat substrates) the lubricant melts, and the solid-sliding regime is destroyed.

When both substrates are curved in the x direction with the same curvature parameters, the ground state of the system corresponds to the five-layer lubricant film with an ideal structure of the layers. The curvatures of the substrates coincide, and the lubricant film just follows the substrates. But when the top substrate moves, one have alternatively, a configuration where the curvatures coincide as in the ground state, and a saddle configuration where the curvatures anti-coincide, so that in one-half of the contact area the film is compressed, while in the other half, the distance between the substrates is much larger than the width of the five-layer lubricant film. Because a thin lubricant film cannot stay free in space but is attracted to one of the substrates, it has to follow either the bottom or top substrate. In simulation we observed that the lubricant indeed takes a ground-state-like configuration when the substrate curvatures coincide, while in the saddle points the lubricant follows the top substrate at the left-hand side, where the z coordinate of the top substrate goes up (so it ''drags'' the lubricant), and at the right-hand side, where the z coordinate of the bottom substrate goes up, the lubricant follows the bottom substrate. Thus, in the middle point the lubricant has to switch between these two configurations, and this decreases the system mobility. The $v_{top}(f)$ dependence for this case is shown in Fig. 15 by down triangles. The backward transition now takes place at $f_b \approx (2-3)\times 10^{-3}$. When the force increases up to $f \sim 0.04$, the film does not have enough time to reach the five-layer ground-state-like configuration between the saddle points. It first takes a six-layer structure but soon (at $f_f \gtrsim 0.04$) the lubricant melts and the sliding is destroyed. Note, however, that the situation described above corresponds to a rare case when the curvature parameters of both substrates are exactly equal to one another. In all other cases, in a given region, only one of the substrates is usually strongly curved.

We also checked the system mobility when the substrates are curved in the y direction (perpendicular to the sliding direction). When only the top substrate is curved, the velocity remains approximately the same as that for the flat substrates (for example, for $f=2\times 10^{-3}$ the velocity decreases from $v \approx 0.98$ for the flat substrates to $v_{top} \approx 0.96$ for the curved top substrate). When both substrates are curved, the velocity remains unchanged (e.g., for $f=2\times 10^{-3}$, the velocity increases to $v_{top} \approx 0.985$). Finally, when the top substrate is curved in both x and y directions simultaneously, the velocity decreases for the $f=2\times 10^{-3}$ case to the value $v_{top} \approx 0.52$ (compare with $v_{top} \approx 0.57$ for the case when the top substrate is curved in x direction only).

Thus, we may conclude that the simulation results obtained for the system with flat substrates stay valid, at least qualitatively, for the curved ones.

IV. DISCUSSION AND CONCLUSIONS

To summarize, we have studied the friction for a thin solid lubricant film between two flat solid substrates and found that the frictional losses are mainly due to the excitation of z vibrations in the lubricant with the washboard frequency. The anharmonicity of lubricant vibrations is found to be important and leads to heating of the lubricant. Thus, a first lesson learned from the simulation of a complex model, is that simple Frenkel-Kontorova-type models with harmonic springs between the atoms cannot describe the kinetic friction properly.

The solid lubricant between two flat (or at least not too rough) substrates provides the smallest possible frictional force for high-speed systems. The energy losses are very small both in the low-velocity (but $v_{top} > v_b \sim 10$ m/s) case, as well as in the high-velocity ($v_{top} \gtrsim v_{sound}$) regime, the latter regime being stable if there is a gap between the lubricant and substrate phonon spectra. If the lubricant film is in a liquid state (melted either due to high substrate temperature or because of very high speed), the frictional force is much larger as seen from Fig. 16. When the lubricant is refrozen from the melted state, it takes an amorphous structure because, due to the contact with the substrates, the energy is removed from the lubricant very quickly, and the confined lubricant film has no time to order. The frictional force in the case of an amorphous lubricant may be even larger than for the melted one (see Fig. 16).

The solid lubricant between flat substrates leads also to quite small values of the static frictional force f_s. This agrees with the results of previous simulations (see Ref. [7] and references therein). The new result of the present paper is the dependence of f_s on the number of layers in the solid lubricant film. The exponential decrease of f_s with N_l may be used for explanation of experimental values of the velocity of the transition from smooth sliding to stick-slip motion as will be discussed below.

We also checked how the results are sensitive to the parameters of the model. First, changing the mass m_S of the top rigid substrate practically does not change the adiabatic

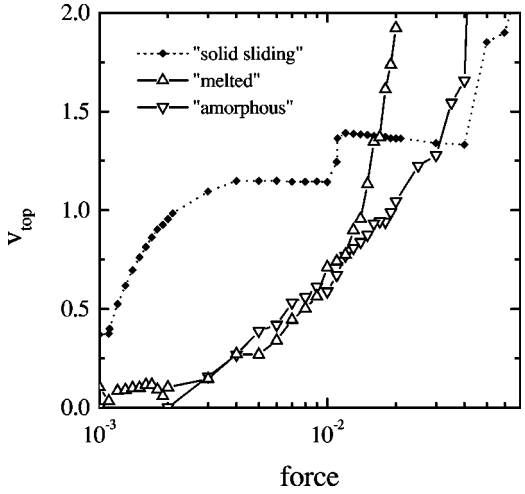

FIG. 16. The $v_{\rm top}(f)$ dependencies for the melted lubricant ($T_{\rm lub}\approx 0.5$, the up triangles) and the frozen (amorphous) lubricant (the down triangles).

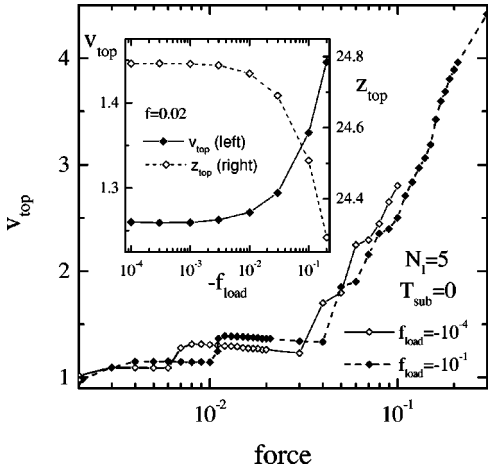

FIG. 17. The dependencies $v_{\rm top}(f)$ for two values of the load $f_{\rm load}=-0.1$ (dashed curve and solid diamonds) and $f_{\rm load}=-10^{-4}$ (solid curve and open diamonds) for the five-layer film at $T=0$. Inset: $v_{\rm top}(f_{\rm load})$ (left axes) and $z_{\rm top}(f_{\rm load})$ (right axes) for the fixed value of the driving force $f=0.02$.

$v_{\rm top}(f)$ dependence, thus the velocity in the steady solid-sliding regime does not depend on m_S. Another important parameter is the minimal external damping $\eta_{\rm min}$ that models the multiphonon and/or ''electron-hole'' contributions to the energy exchange of lubricant with substrates. We found that the results are approximately unchanged for $v_{\rm top}\gtrsim 1$, when the energy losses inside the lubricant play the main role. At small forces velocities, when $v_{\rm top}\lesssim 1$, the values of $v_{\rm top}$ and $z_{\rm top}$ are larger for smaller values of $\eta_{\rm min}$ and agree with the ''perfect-sliding'' dependence (25).

Finally, let us discuss the relation of the microscopic simulations of the present paper to macroscopic friction.

Dependence on load. We varied $f_{\rm load}$ to test the Amontons first law $F_{\rm fric}=\mu F_{\rm load}$, where μ (called the friction coefficient by tribologists) should be approximately constant. For example, the simulation results for a much lower load $f_{\rm load}=-10^{-4}$ than that used in all simulation presented above, are shown in Fig. 17. The trivial result is that the width of lubricant increases with decreasing of $f_{\rm load}$. Therefore, the external damping coefficient, which exponentially depends on z, decreases with $f_{\rm load}$. As a result the backward transition now takes place at a lower force $f=f_b\approx(3-4)\times 10^{-5}$ when $v_b\lesssim 3\times 10^{-2}$. The forward transition also occurs earlier, at $f_f\approx 0.1-0.11$ when $v_b\lesssim 3$. For $v_{\rm top}\gtrsim 1$ the dependence $v_{\rm top}(f)$ is approximately the same as that for the high load, while for lower forces when $v_{\rm top}<1$, the values of $v_{\rm top}$ for the same values of f are larger than those for the $f_{\rm load}=-0.1$ case, because the external friction is smaller due to larger values of z. The dependencies of $v_{\rm top}$ and $z_{\rm top}$ on $f_{\rm load}$ for a fixed value of the dc force $f=0.02$, are shown in the inset of Fig. 17. Surprisingly, $v_{\rm top}$ is not decreasing but increases when $f_{\rm load}$ increases, because for the chosen value of the dc force, a resonance effect plays a role (the washboard frequency penetrates into the lubricant phonon spectrum). In general, however, the variation of $f_{\rm load}$ results in a little change only. This confirms once more that the empirical Amontons first law works due to change of the contact area with load [1]. On the contrary, He and Robbins [20] have found that the frictional force is directly proportional to the load. However, their simulation was done with the const-v algorithm at low velocities ($v_{\rm top}<0.1$ nu) and much higher temperatures than those studied in our simulations. Besides, the authors of Eq. [20] used the Langevin equations with a constant external damping.

Dependence of results on the interaction parameters. Above we have studied the system behavior for the fixed set of parameters, when the interaction within the lubricant, $V_{ll}=1$, is much larger than the interaction of the lubricant with substrates, $V_{sl}=1/3$. For these parameters the solid-sliding regime had indeed to be expected. Below we present a few simulation results for other sets of parameters.

First, let us consider the case with $V_{ll}=V_{sl}=1/3$, in which the interaction within the lubricant has the same magnitude as the lubricant-substrate interaction. In fact, this case is similar to that studied above, because an effective lubricant-substrate interaction is again smaller than the interaction within the lubricant due to mismatch of the substrate lubricant lattice constants. However, an essential new feature of the present case is that now the phonon frequencies of the lubricant are smaller. Because the interaction within the substrates and within the lubricant differs by nine times, the substrate and lubricant phonon spectra are well separated one from another even for the five-layer lubricant film as shown, for example, in the inset of Fig. 18 for the z component. There is a wide gap for the frequencies $4<\omega<6.5$, where the density of phonon states is very small. Thus, one could expect that if the washboard frequency comes into this frequency interval, the effective friction should be small, and the solid-sliding regime will persist up to very high velocities. Indeed, the simulation results for the one-layer lubricant film presented in Fig. 18, show that the solid-sliding regime indeed survives now until the very high force ($f_f\gtrsim 5$) and velocity ($v_f\approx 10$). This effect is similar to the ''re-entrant'' transition observed by Stevens and Robbins [17], where with the increase of the driving velocity the lubricant melts but

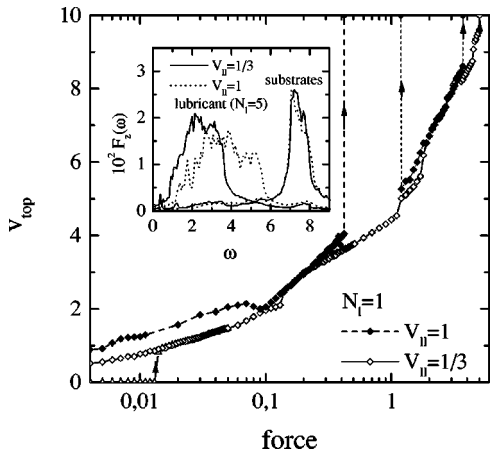

FIG. 18. The $v_{\mathrm{top}}(f)$ dependence for the one-layer lubricant with the interatomic interactions $V_{ll}=1/3$ (solid curve and open diamonds) compared with that for the $V_{ll}=1$ case (dashed curve and solid diamonds). Inset: the $V_{ll}=1/3$ (solid curves) and $V_{ll}=1$ (dotted curves) spectra for the five-layer lubricant.

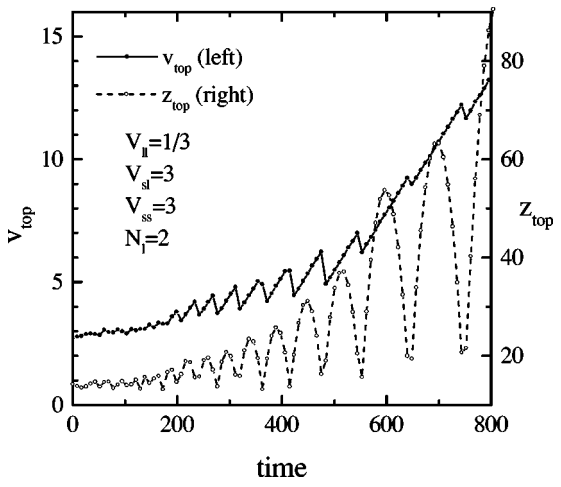

FIG. 19. Beginning of motion for the ''glued'' two-layer lubricant film ($V_{ss}=V_{ls}=3$, $V_{ll}=1/3$).

then, at a higher velocity, it solidifies again. In our simulation with a small external damping we did not obtained melting but instead observed a large increase of the lubricant temperature. For velocities $v_{\mathrm{top}}>3$ (recall that in the previous case the solid-sliding regime was already destroyed at so high velocities) the washboard frequency is higher than the lubricant phonon frequencies, thus the excitation of oscillations in the lubricant as well as the effective lubricant temperature decrease. This regime corresponds to the ''flying'' one, i.e. The decoupling of phonon spectra of the lubricant and the substrates stabilizes the ''flying'' state. With increasing dc force the lubricant remains sliding in a solid state, while the amplitude of the z oscillations of the substrate atoms strongly increases at $v_{\mathrm{top}}>6$, and this finally destroys the solid-sliding regime. Note that for the forces $0.1<f<0.4$, when $2<v_{\mathrm{top}}<3$, the system behavior is similar to that described above, because the densities of lubricant vibrations are similar at these washboard frequencies. At smaller forces, $f<0.1$, the effective friction as well as the lubricant temperature are larger for the weak-lubricant case than those for the previous case. The backward transition to the locked state takes place now at $f_b \lesssim 0.003$, when $v_b \approx 0.15$. The static frictional force, $f_s \approx 0.013-0.014$, is also smaller than that for the previous case (recall $f_s \approx 0.02$ for the $V_{ll}=1$ case). Note, however, that we observed the ''flying'' regime only for the one-layer film. For the five-layer lubricant the forward transition takes place at $f_f \approx 0.025-0.026$, i.e., much earlier than for the $V_{ll}=1$ case, and the attempts to get a high-velocity regime failed. Note that although it seems quite unusual to have a velocity close to the sound speed in real machines, the ''flying'' regime may be reached in, e.g., next generation of hard-disk drives. In a disk with a radius of 4 cm and a rotating speed of 10 000 rpm, the speed of the head with respect to the plateau already exceeds 40 m/s, i.e., the crash of the head on the plateau in a failure is an example of high-speed friction, although, unfortunately, the ''flying'' regime would not be reached by the current generation of hard disks.

Second, we studied the opposite case, in which the lubricant-substrate interaction is much larger than the interaction within the lubricant, namely, $V_{sl}=3$ and $V_{ll}=1/3$. In this case the two utmost lubricant layers tend to be attached to the corresponding substrates, so a sliding can only emerge inside the lubricant. In fact, this situation is close to real oil lubricant, where the interaction with substrates prevents the lubricant from being squeezed out from the contact areas. In the case of $N_l=2$, all lubricant atoms are attached by the substrates, so there is no ''lubricant'' between the two sliding ''bodies,'' each consisting of the rigid substrate with one attached *s* layer and one ''glued'' layer of *l* atoms. Thus, the situation is close to the dry friction for two commensurate perfectly aligned substrates. However, the interaction between the bodies, $V_{ll}=1/3$ is much smaller than the interaction inside them, where $V_{ss}=V_{sl}=3$. In this case at some critical force, $f_s \sim 0.08$, the bodies decouple one from another, the distance between them increases, and they begin to ''fly'' almost without friction. But the loading force pushes the bodies into contact again, so they collide and almost elastically repulse, then again collide, etc. The motion of the top substrate resembles a series of jumps as shown in Fig. 19. If the driving force remains constant, the amplitude of jumps increases with time, and finally at one collision the surface lubricant layers are destroyed.

For a thicker lubricant film, $N_l>2$, there are weakly interacting lubricant atoms between the two bodies. Note that for these parameters in the ground-state configuration the topmost lubricant layers that are attached to the substrates, have slightly more atoms than the middle layer(s). When the motion begins at $f=f_s$ in this case (e.g., for the $N_l=3$ or $N_l=5$ system $f_s \sim 0.03-0.07$), the middle lubricant layers melt according to a three-dimensional (3D) melting mechanism (one layer in the $N_l=3$ system or three layers for the $N_l=5$ case), and the width of the lubricant film increases. Starting with the configuration just after the beginning of the motion (e.g., that for $f=0.08$ for the $N_l=5$ system), we abruptly decreased the dc force to a smaller value. The results are presented in Fig. 20. If $f \leqslant 0.01$, the motion locks in the five-layer solid state, while for $f \geqslant 0.02$ the top body is

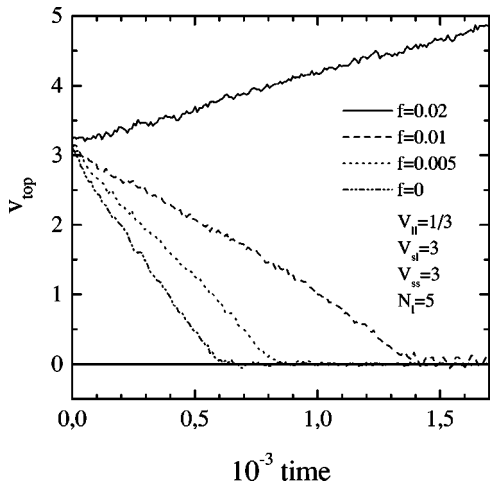

FIG. 20. Motion of the ''glued'' five-layer lubricant film ($V_{ss}=V_{ls}=3$, $V_{ll}=1/3$) for different driving forces.

''flying'' and its velocity increases linearly with time. Thus, the frictional force for a melted lubricant in this system is $f_{\mathrm{fric}}\sim 0.015$.

Third, all the scenarios described above were obtained for the model where the external damping depends on the distance from the substrates and, thus, it is very small for the middle lubricant layer(s). However, if we change the model in the way that the minimal external damping would not depend either on distance or on velocity, the scenario changes to that already observed in the previous works [16,22] and described in the Introduction. Now when the sliding begins the width does not increase significantly and the sliding steady state survives with increasing the dc force. With increasing force, the middle layers melt due to sliding according to a 2D melting mechanism, i.e., the lubricant keeps its layered structure and different lubricant layers slide one over another. This model may be applied to lubricants with complex molecules like organic ones, where an internal viscosity of the lubricant plays an important role.

The transition from smooth sliding to stick-slip motion. If, instead of a constant dc force we would drive the system through a spring attached to a stage moving with the velocity v_{top}, the system would exhibit a transition from smooth sliding to stick-slip motion at the velocity $v_{\mathrm{top}}\approx v_b$ [28]. A similar result would be expected with a large enough substrate block so that its elasticity would start playing a role. Experimentally the transition from smooth sliding to stick-slip motion is observed in almost all systems where the static friction force is nonzero (the zero f_s corresponds to liquid lubricant). There are at least three mechanisms that can explain the transition from smooth to stick-slip motion: (a) ''inertia'' mechanism, when the backward sliding-to-locked transition occurs at the force $f_b<f_s$ due to inertia of the moving lubricant in the underdamped system (this mechanism was discussed above in Sec. III C); (b) ''melting-freezing'' mechanism [16,2,3,10], when the lubricant undergo dynamical phase transitions between a fluidized state during slip (sliding) and a solid state during stick; and (c) ''memory'' mechanism (e.g., see Refs. [2,3,5]), when, after the sliding-to-locked transition, the static friction force increases with the time of stationary contact. The simulation results of the present paper show that the ''inertia'' mechanism leads to the critical velocity $v_c\sim 10^{-2}$ nu$\approx$10 m/s, and we do not see any reason to get a much lower value for v_c. This value is orders of magnitude larger than the experimental value, which rules out the inertia mechanism to explain the experimentally observed stick slip to smooth sliding transition. For the model parameters used in the present paper, we also did not observe the melting of thin lubricant films except for extremely large forces and velocities. The lubricant may melt at $f>f_s$ if it is strongly coupled with the substrates or, in a more specific case, when the lubricant is perfectly commensurate and aligned with the substrates [16,28]. But, in such situations, when the driving force is reduced, the lubricant quickly solidifies again due to a fast energy exchange with the substrates (as discussed above in Sec. III D), and the backward transition to the locked state takes place at the velocity $v_c\sim 1$ nu [16,36,28]. Thus, in this case too, the top substrate cannot move smoothly with a low velocity at the microscopic scale. In experiments the transition from stick slip to smooth motion is observed usually at a velocity $v_c\sim 1$ μm/s$\approx 10^{-9}$ nu [4]. Even if we suppose that there are only few contacts (asperities) between the solids and only one of the contacts moves at a time, we do not see a way by which the macroscopic stick-slip to smooth transition could be explained by the microscopic (atomic-scale) mechanisms. Thus, we conclude that the mechanism responsible for the experimentally observed stick-slip to smooth transition, at least for ''simple'' lubricant molecules, should be the ''memory'' effects. After the sliding-to-locked transition, the static friction force increases with time due to plastic deformation of the lubricant, for example, because of an increase of the area of real contact, or due to the decrease of the lubricant width (according to the simulation results of the present paper, the squeezing of the lubricant leads to the increase of f_s), or due to interdiffusion of lubricant molecules between different layers of the lubricant in the case of a lubricant consisting of long-chain polymers. All these processes involve plastic deformations and thus are characterized by macroscopic-scale characteristic times. Then, the experimentally observed velocities of the transition from smooth sliding to stick-stick motion can be explained with the help of earthquakelike models [37–39] as was demonstrated in Refs. [3,40,41,28]. Consequently the analysis of the order of magnitude of the stick-slip to smooth-sliding transition velocity suggests that the explanation of this penomenon should not be seeked at the microscopic scale and is probably out of reach of current molecular-dynamics simulations. Besides, this also explains why the experimentally measured kinetic friction in the smooth sliding regime is often almost independent of the velocity, while the microscopic one shows a very strong dependence. Indeed, if the macroscopic smooth sliding corresponds to the microscopic stick-slip regime, the macroscopic kinetic friction would correspond to microscopic static friction force, which is constant. Therefore the evaluation of the orders of magnitude that we made in this paper lead us to conclude that there is a fundamental difference between microscopic friction and the macroscopic experimental properties. This should perhaps be

considered for the current projects to build micromachines.

Finally, in real experimental systems the rate of change of the driving force corresponds to adiabatically slow variation of f in simulations. Therefore, to obtain reliable results, which do not depend on an initial configuration, it is important to reach the steady state for a given f. As observed in the present paper, lubricant systems are often characterized by quite long relaxation times $\tau_{\rm relax} > 10^3$ nu$\approx 10^{-10}$ s (or even $\tau_{\rm relax} \gg 10^{-10}$ s in the solid-sliding regime at velocities $v_{\rm top} < 10$ m/s). In simulations for large systems with realistic interactions one could expect to reach the stationary state for one given set of parameters (including the value of the driving force) only, and not for adiabatically changing force. Thus, although being very attractive, the ''millions of atoms'' simulations hardly could give reliable values for the kinetic friction in their present stage. This is why we believe ''simple'' models are still very important. But they must also be taken with great caution because, as we have shown in the present paper, the results obtained with simple models may also strongly depend on the model chosen, in particular on the damping introduced in the simulations. We tried here to introduce a damping mechanism motivated by microscopic considerations and we showed that the results are sometimes very different from those given by a uniform damping coefficient as often considered.

ACKNOWLEDGMENTS

We wish to express our gratitude to A. R. Bishop, B. N. J. Persson, J. Röder, and M. Urbakh for helpful discussions. This research is supported in part by NATO Grant No. HTECH.LG.971372. O.B. was also partially supported by INTAS Grant No. 97-31061.

[1] F. P. Bowden and D. Tabor, *The Friction and Lubrication of Solids* (Clarendon Press, Oxford, 1986).

[2] B. N. J. Persson, *Sliding Friction: Physical Principles and Applications* (Springer-Verlag, Berlin, 1998).

[3] B. N. J. Persson, Surf. Sci. Rep. **33**, 83 (1999).

[4] C. M. Mate, in *Handbook of Micro/Nano Tribology*, edited by B. Bhushan (CRC Press, Boca Raton, 1995) p. 167.

[5] *Fundamentals of Friction: Macroscopic and Microscopic Processes*, edited by I. L. Singer and H. M. Pollock (Kluwer, Dordrecht, 1992); *Physics of Sliding Friction*, edited by B. N. J. Persson (Kluwer, Dordrecht, 1996).

[6] G. Reiter, A. L. Demirel, and S. Granick, Science **263**, 1741 (1994); B. Brushan, J. N. Israelachvili, and U. Landman, Nature (London) **374**, 607 (1995); A. D. Berman, W. A. Ducker, and J. N. Israelachvili, Langmuir **12**, 4559 (1996).

[7] M. O. Robbins, in *Jamming and Rheology: Constrained Dynamics on Microscopic and Macroscopic Scales*, edited by A. J. Liu and S. R. Nagel (Taylor and Francis, London, 2000); M. O. Robbins and M. H. Müser, in *Handbook of Modern Tribology*, edited by B. Bhushan (CRC Press, Boca Raton, 2000).

[8] J. Gao, W. D. Luedtke, and U. Landman, J. Phys. Chem. B **101**, 4013 (1997); *ibid.* **106**, 4309 (1997).

[9] J. E. Hammerberg, B. L. Holian, J. Röder, A. R. Bishop, and S. J. Zhou, Physica D **123**, 330 (1998); R. P. Mikulla, J. E. Hammerberg, P. S. Lomdahl, and B. L. Holian, Mater. Res. Soc. Symp. Proc. **522**, 385 (1998).

[10] B. N. J. Persson, Phys. Rev. Lett. **71**, 1212 (1993); Phys. Rev. B **48**, 18 140 (1993); J. Chem. Phys. **103**, 3849 (1995).

[11] O. M. Braun, T. Dauxois, M. Paliy, and M. Peyrard, Phys. Rev. Lett. **78**, 1295 (1997); O. M. Braun, T. Dauxois, M. Paliy, and M. Peyrard, Phys. Rev. E **55**, 3598 (1997); M. Paliy, O. Braun, T. Dauxois, and B. Hu, *ibid.* **56**, 4025 (1997).

[12] M. Weiss and F.-J. Elmer, Phys. Rev. B **53**, 7539 (1996); Z. Phys. B: Condens. Matter **104**, 55 (1997); O. M. Braun, A. R. Bishop, and J. Röder, Phys. Rev. Lett. **79**, 3692 (1997); O. M. Braun, B. Hu, A. Filippov, and A. Zeltser, Phys. Rev. E **58**, 1311 (1998).

[13] M. G. Rozman, M. Urbakh, and J. Klafter, Phys. Rev. Lett. **77**, 683 (1996); Phys. Rev. E **54**, 6485 (1996); Europhys. Lett. **39**, 183 (1997).

[14] G. He, M. H. Müser, and M. O. Robbins, Science **284**, 1650 (1999); M. H. Müser and M. O. Robbins, Phys. Rev. B **61**, 2335 (2000); M. H. Müser, L. Wenning, and M. O. Robbins, Phys. Rev. Lett. (to be published); e-print cond-mat/0004494.

[15] J. Gao, W. D. Luedtke, and U. Landman, J. Chem. Phys. **106**, 4309 (1997).

[16] P. A. Thompson and M. O. Robbins, Science **250**, 792 (1990); M. O. Robbins, and P. A. Thompson, *ibid.* **253**, 916 (1991).

[17] M. J. Stevens and M. O. Robbins, Phys. Rev. E **48**, 3778 (1993).

[18] P. A. Thompson, G. S. Grest, and M. O. Robbins, Phys. Rev. Lett. **68**, 3448 (1992); P. A. Thompson, M. O. Robbins, and G. S. Grest, Isr. J. Chem. **35**, 93 (1995); A. Baljon and M. O. Robbins, MRS Bull. **22**, 22 (1997).

[19] M. Cieplak, E. D. Smith, and M. O. Robbins, Science **265**, 1209 (1994); E. D. Smith, M. O. Robbins, and M. Cieplak, Phys. Rev. B **54**, 8252 (1996).

[20] G. He and M. O. Robbins, Tribol. Lett. (to be published); e-print cond-mat/0008196.

[21] O. M. Braun, T. Dauxois, and M. Peyrard, Phys. Rev. B **56**, 4987 (1997).

[22] O. M. Braun, A. R. Bishop, and J. Röder, Phys. Rev. Lett. **82**, 3097 (1999).

[23] M. Hirano and K. Shinjo, Phys. Rev. B **41**, 11 837 (1990).

[24] M. R. Sørensen, K. W. Jacobsen, and P. Stoltze, Phys. Rev. B **53**, 2101 (1996).

[25] P. Ballone and B. N. J. Persson, J. Chem. Phys. (to be published).

[26] J. Krim, D. H. Solina, and R. Chiarello, Phys. Rev. Lett. **66**, 181 (1991); J. Krim and R. Chiarello, J. Vac. Sci. Technol. A **9**, 2566 (1991).

[27] C. W. Gardiner, *Handbook of Stochastic Methods* (Springer-Verlag, Berlin, 1983).

[28] O. M. Braun (unpublished).

[29] J. W. Gadzuk and A. C. Luntz, Surf. Sci. **144**, 429 (1984); P. Avouris and B. N. J. Persson, J. Phys. Chem. **88**, 837 (1984);

D. C. Langreth, Phys. Scr. **35**, 185 (1987); R. G. Tobin, Surf. Sci. **183**, 226 (1987).

[30] O. M. Braun, A. I. Volokitin, and V. P. Zhdanov, Usp. Fiz. Nauk **158**, 421 (1989) [Sov. Phys. Usp. **32**, 605 (1989)].

[31] O. M. Braun, Surf. Sci. **213**, 336 (1989); O. M. Braun and A. I. Volokitin, Fiz. Tverd. Tela (Leningrad) **28**, 1008 (1986) [Sov. Phys. Solid State **28**, 564 (1986)].

[32] B. N. J. Persson, Phys. Rev. B (to be published).

[33] A. R. Bishop, O. M. Braun, M. V. Paliy, and J. Röder, Phys. Rev. E (to be published).

[34] J. B. Sokoloff, Phys. Rev. B **42**, 760 (1990); **42**, 6745(E) (1990); B. N. J. Persson and A. Nitzan, Surf. Sci. **367**, 261 (1996); J. B. Sokoloff and M. S. Tomassone, Phys. Rev. B **57**, 4888 (1998).

[35] H. Risken, *The Fokker-Planck Equation* (Springer-Verlag, Berlin, 1984).

[36] B. N. J. Persson, Phys. Rev. B **50**, 4771 (1994).

[37] R. Burridge and L. Knopoff, Bull. Seismol. Soc. Am. **57**, 3411 (1967).

[38] J. H. Dieterich, J. Geophys. Res. **84**, 2169 (1979); A. Ruina, *ibid.* **88**, 10 359 (1983); J. R. Rice and A. L. Ruina, J. Appl. Mech. **50**, 343 (1983); J. C. Gu, J. R. Rice, A. L. Ruina, and S. T. Tse, J. Mech. Phys. Solids **32**, 167 (1984).

[39] J. M. Carlson, J. S. Langer, and B. E. Shaw, Rev. Mod. Phys. **66**, 657 (1994).

[40] B. N. J. Persson, Phys. Rev. B **51**, 13 568 (1995).

[41] B. N. J. Persson, Phys. Rev. B **55**, 8004 (1997).